

©Copyright 2021

Melanie Joyce Anderson

Integrating natural and synthetic systems for airborne bio-hybrid
chemical sensing devices

Melanie Joyce Anderson

A dissertation
submitted in partial fulfillment of the
requirements for the degree of

Doctor of Philosophy

University of Washington

2021

Reading Committee:

Sawyer B Fuller, Chair

Thomas L Daniel, Chair

Santosh Devasia

Program Authorized to Offer Degree:
Mechanical Engineering

University of Washington

Abstract

Integrating natural and synthetic systems for airborne bio-hybrid chemical sensing devices

Melanie Joyce Anderson

Co-Chairs of the Supervisory Committee:

Professor Sawyer B Fuller

Mechanical Engineering

Professor Thomas L Daniel

Biology

Chemical sensing is a universal capability of living organisms across all scales and taxa. Most animals depend on this ability for their survival and flying animals have evolved sophisticated sensing capabilities and olfactory search behaviors that allow them to efficiently search in highly complex 3D environments such as the forest canopy, which include myriad obstacles and turbulent flow. The ability to sense complex organic molecules with extremely small concentrations (parts per trillion) is far beyond the capabilities of even state of the art portable synthetic sensors. In this work, we have developed a portable biohybrid chemical sensor which uses an antenna from the *Manduca sexta* moth to detect various chemicals. Additionally we have shown that this biohybrid chemical sensor can also be used on a human-safe palm-sized air vehicle. Using this sensor along with a suite of additional navigational sensors, as well as passive wind fins, this robot orients upwind and navigates autonomously toward the source of airborne plumes. This robot is the first flying biohybrid system to successfully perform odor localization in a confined space, and it is able to do so while detecting and avoiding obstacles in its flight path. We show that insect antennae respond more quickly than metal oxide gas sensors, enabling odor localization at an improved speed over previous flying robots.

TABLE OF CONTENTS

	Page
List of Figures	ii
List of Tables	iii
Introduction	1
Chapter 1: The Smellicopter, a bio-hybrid odor localizing nano air vehicle	2
1.1 Introduction	3
1.2 System components	6
1.3 Demonstration	13
1.4 Conclusion	15
Chapter 2: A bio-hybrid odor-guided autonomous palm-sized air vehicle	18
2.1 Introduction	19
2.2 Design and system architecture	23
2.3 Results	30
2.4 Discussion	35
Chapter 3: A pocket-sized bio-hybrid chemical detector for use in research, teaching, and industry	38
3.1 Introduction	39
3.2 Applications	41
3.3 SmellPhone design	42
3.4 Results	44
Bibliography	48
Appendix A: Where to find the files	52

LIST OF FIGURES

Figure Number	Page
1.1 The Smellicopter	4
1.2 The electroantennogram	6
1.3 Electroantennogram Analog Schematic	7
1.4 EAG model magnitude response	8
1.5 The EAG response to a hand puffed stimulus	9
1.6 System architecture diagram	11
1.7 Cast and surge state machine	12
1.8 Tests of the Smellicopter performing an olfactory search in a wind tunnel . .	14
2.1 Anatomy and control architecture of the “Smellicopter”	24
2.2 Flow Chart of the cast-and-surge algorithm	28
2.3 Electroantennograms from a moth antenna and signals from metal oxide sensors	31
2.4 Odor localization trials	32
2.5 Obstacle avoidance trials	35
3.1 The SmellPhone	40
3.2 The SmellPhone connected to a cell phone	41
3.3 Antenna response to floral scent over time	43
3.4 The SmellPhone circuitry	44
3.5 The automated odor delivery system	45
3.6 A comparison of our electroantennogram (EAG) sensor vs a commercial metal oxide (MOX) sensor	46

LIST OF TABLES

Table Number	Page
1.1 Chemical composition of floral scent	10
2.1 EAG vs MOX comparison	31
2.2 Summary data for odor localization trials	34
3.1 Chemical source amounts	45

ACKNOWLEDGMENTS

There are many who helped me along the way on this journey. I want to take a moment to thank them.

First, I wish to thank my advisors, Tom Daniel and Sawyer Fuller, who have welcomed, encouraged, and aided me all along the way. Without them, I would not have made it.

To my friends, my parents, and my sister: thank you for your never-ending love and support.

Finally, to my partner, Joseph, you have helped me in more ways than I can say. This is truly just as much your accomplishment as it is mine. It is time to celebrate; you earned this degree right along with me.

INTRODUCTION

Nature has evolved a myriad of chemical sensors that are lighter and faster and more sensitive than products on the market. For example, the acute sense of smell and intelligence of dogs allows them to find drugs and bombs better than any robotic system. Many flying insects, although they are tiny, also have an incredible ability to detect volatile organic compounds that vastly exceeds the capabilities of portable chemical detectors.

The antennae of tobacco hornworm moths (*Manduca sexta*) are like a nose: moths use them to locate food, avoid predators, and find mates by detecting miniscule chemical signatures in the air. Using electronics to measure the electrical activity in the antennae as it reacts to odors is called an electroantennogram (EAG).

During this work, a miniaturized EAG was designed and integrated with a palm-sized drone platform. This integrated platform is equipped with additional sensors and is programmed to autonomously perform a bio-inspired search algorithm to follow a chemical plume to its source, even in the presence of obstacles.

Additionally, a modified version of the biohybrid sensor was developed to be able to interface with a mobile phone for portable electroantennograms outside of a drone application. This version was tested against a state-of-the-art metal oxide (MOX) sensor with various chemicals.

Chapters 1 and 2 of this document consist of two peer-reviewed publications detailing this work. Chapter 3 is a paper which will be submitted to a scientific conference.

Chapter 1

THE SMELLICOPTER, A BIO-HYBRID ODOR LOCALIZING NANO AIR VEHICLE

Melanie J. Anderson¹, Joseph G. Sullivan², Jennifer L. Talley³, Kevin M. Brink⁴,
Sawyer B. Fuller⁵, and Thomas L. Daniel⁶

Chapter 1 is a publication at the 2019 IEEE/RSJ International Conference on Intelligent Robots and Systems (IROS) in Macau, China, November 4-8, 2019.

The main contributions of this work are showing **proof-of-concept** demonstrations of the 1) miniaturized electroantennogram sensor, 2) integration with a palm-sized drone platform, and 3) insect-inspired search strategy.

*This work was supported by AFCOE NIFTI: Nature Inspired Flight Technologies and Ideas.

¹Melanie Anderson is with the Department of Mechanical Engineering, University of Washington, Seattle, WA 98195

²Joseph Sullivan is with the Department of Electrical Engineering, University of Washington, Seattle, WA 98195

³Jennifer Talley is a research biological scientist at the Air Force Research Laboratory, Eglin AFB, FL 32542

⁴Kevin Brink is the senior research engineer at the Air Force Research Laboratory, Eglin AFB, FL 32542

⁵Sawyer Fuller is a professor in the Department of Mechanical Engineering, University of Washington, Seattle, WA 98195

⁶Tom Daniel is a professor in the Department of Biology, University of Washington, Seattle, WA 98195

Abstract

Robotic airborne chemical source localization has critical applications ranging from search and rescue to hazard detection to pollution assessment. Previous demonstrations on flying robots have required search times in excess of ten minutes, or required computation-intensive signal processing, largely because of the slow response of semiconductor gas sensors. To mitigate these limitations, we developed a hybrid biological/synthetic chemical sensing platform consisting of a moth antenna on an aerial robot. We demonstrate that our robot, a 9 centimeter nano drone, can repeatedly detect and reach the source of a volatile organic chemical plume in less than a minute. We also introduce wind vanes to passively aim the robot upwind, greatly simplifying control. To our knowledge this is the first odor-finding robot to use this approach, and it allows for localization using feedback only from sensors carried on-board rather than GPS, allowing indoor operation. The chemical sensor consists of a hybrid biological/synthetic integrated chemical sensor (electroantennogram) using an excised antenna of the hawkmoth *Manduca sexta* and associated miniaturized electrophysiology conditioning circuitry. Our robot performs an insect-inspired cast-and-surge search algorithm inspired by the odor-tracking behavior observed in *Manduca sexta*. These results represent a significant step toward robots that have the speed and sensitivity of biological systems.

1.1 Introduction

Chemical gas sensors are used in many situations where human safety is at risk, either to help locate trapped persons in natural disasters, or to detect the presence of dangerous chemicals in the environment. For example, chemical sensors could be used in earthquake zones for locating survivors, in industrial facilities to monitor the concentration of toxic chemicals or to detect hazardous leaks, or urban conflict areas to detect explosives or chemical warfare agents. In situations such as these there is a need for autonomous systems or robots with chemical sensing capabilities, either to supplement limited human resources in search and rescue efforts, or for operating in environments that are too toxic or dangerous for people to enter.



Figure 1.1: The Smellicopter is a modified commercial Crazyflie drone with custom electroantennogram circuit and wind fins for passive upwind orientation.

Chemosensing robots require three distinguishing elements: a robotic platform with maneuvering and navigation capability, a sensor that can detect a particular volatile chemical, and an olfactory search strategy. In order for a chemosensing robot to be effective, the robot must be designed with the characteristics of its operating environment in mind. Also, its sensor must be selective for a chemical that is relevant to its task. In many cases, the operating environment of the robot will include confined spaces and unpredictable terrain which impede terrestrial robots.

Unmanned aerial vehicles (UAVs) are attractive platforms for building chemosensing robots because they can navigate in complex 3D environments without the challenges of difficult terrains.

Recently there have been demonstrations of multi-rotor UAVs performing olfactory searches with differing search strategies and using metal oxide gas sensors. Neumann et al [1] presented an outdoor olfactory search on a 1 m diameter quadrotor using both a bio-inspired strategy, and a particle filter strategy. Additionally, Luo et al [2] demonstrated an indoor olfactory search using a UAV slightly larger than the commercial Crazyflie drone that could infer the direction of a gas source in the robot's inertial frame calculated using data from three metal oxide sensors.

A limitation of metal oxide sensors is that they have slow response times and large refractory periods in the presence of high gas concentrations [3], which requires long pauses of about 20 seconds at each location for the sensor reading to stabilize. Luo's method avoided these long pauses by performing many thousands of calculations each second using an off-board computer with a powerful desktop GPU [2]. Such solutions may challenge small UAVs that are suitable for operation in confined spaces because they are powered by small batteries and can carry only limited payloads. Slow olfactory searches may be impractical, and complex computations require specialized hardware which comes at a cost to both power and weight. Building an autonomous UAV with olfactory search capability in real world conditions remains an ongoing challenge.

In contrast to synthetic systems, many living organisms have evolved highly effective and efficient chemical sensing capability and olfactory search behaviors which are vital to tasks such as locating mates and food [4]. For example, male moths can track females over great distances and detect female pheromones at concentrations far less than parts per trillion [5]. Biological odor detectors, such as moth antennae in electroantennogram preparations, offer a faster response and more sensitive discrimination than is possible with current engineered chemical sensors. To be used in specialized applications, *Manduca sexta* and many other insect species have the potential to be genetically edited by using CRISPR to engineer the sensitivity to specific odors.

This work presents an autonomous hybrid bio-synthetic UAV that uses living tissue to detect chemical gas and performs an olfactory search that mimics the behavior of flying insects. The system detects the presence of particular chemicals using an electroantennogram on an excised moth antenna. This approach provides highly sensitive, selective, fast responding sensing capability at low weight and low power. The olfactory search is performed using a reactive strategy called cast-and-surge that guides the UAV upwind to the gas source. Upwind flying is achieved passively using aerodynamic wind vanes and reduced yaw control authority. This wind-driven passive orientation results in a system which reacts quickly to chemical signals with minimal computational requirements and using all onboard sensing. To the best of our knowledge, this system is the smallest and lowest power chemosensing robot ever demonstrated.

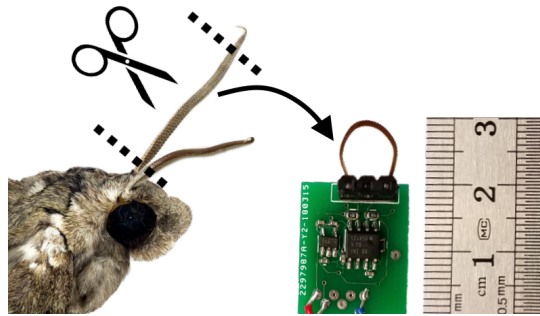


Figure 1.2: The electroantennogram (EAG) is comprised of a single excised antenna from a *Manduca sexta* hawkmoth and our custom signal conditioning circuitry. Our electroantennogram circuit board has a footprint of less than 3 cm².

1.2 System components

1.2.A Electroantennogram

An electroantennogram is an analog circuit that measures the response of a living biological antenna to chemical or mechanical stimulus. These antennae serve as critical sensory organs for insects and other arthropods. In addition to their capacity to sense wind and vibrations, antennae most notably provide olfactory information to the insect to find food and mates [6]. Chemical sensing follows from a complex cascade of molecular interactions. Volatile compounds diffuse into the interior of the antenna where they then bind to odor binding proteins. Those complexes then bind to, and activate, G-protein receptor molecules on the membranes of chemosensory neurons populating the interior of the antenna. Once activated, G-protein mediated pathways provide a whole cell response that greatly amplifies the influence of a single odorant. That amplified response yields an action potential that propagates down the antenna to the brain of the insect. An electroantennogram measures the aggregate electrical activity of the olfactory neurons in an antenna by measuring the voltage drop across the antenna.

One method for producing an electroantennogram is to remove the antenna from the moth and insert wires into both the base and the tip of the antenna. We have observed that

antennae from the *Manduca sexta* hawkmoth in this preparation will continue to produce a signal for up to four hours, but the signal strength will continuously decline over this period. This decline has been recorded in the excised antenna of *Agrotis ipsilon* [7]. Antennal signals can also be captured by probing the brain of the insect and the tip of a single antenna to measure individual neuronal responses [7]; however, this requires additional processing of the spike rate rather than the simple thresholding of a local field potential that we can apply for our electroantennogram.

The electroantennogram (EAG) requires an analog device that amplifies the voltage across an antenna preparation and filters the signal so that it can be measured by an analog to digital converter (ADC). EAGs have been shown to respond faster than metal oxide sensors [3], and are suitable for detecting the presence of chemical gas at a rate of up to 10 Hz [3]. Our EAG design outputs a signal between zero and three V so that signal can be measured by the ADC of many common microcontrollers. The basic elements of the EAG are 1) a high gain preamplifier 2) an active bandpass filter and 3) an output amplifier, which are shown in Fig. 3.4. The EAG weighs just 1.5 g and consumes only 2.7 mW of electrical power. *Manduca sexta* moths are cold anesthetized prior to removing antennae by being placed on ice for at least 15 minutes. For the antenna preparation, we use an excised

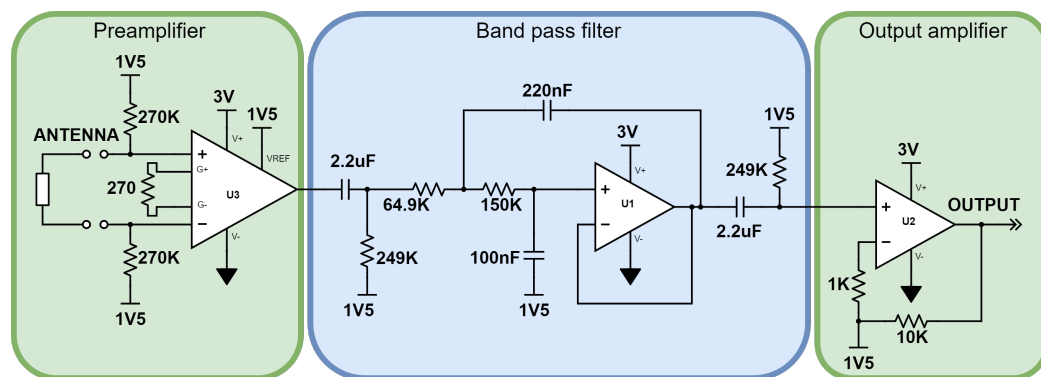


Figure 1.3: Electroantennogram Analog Schematic. The EAG is comprised of three stages, a preamplifier stage, a filtering stage, and an output amplifier stage. Preamplifier U3 part number is INA118, and the part number of op amps U1 and U2 are TLV2333.

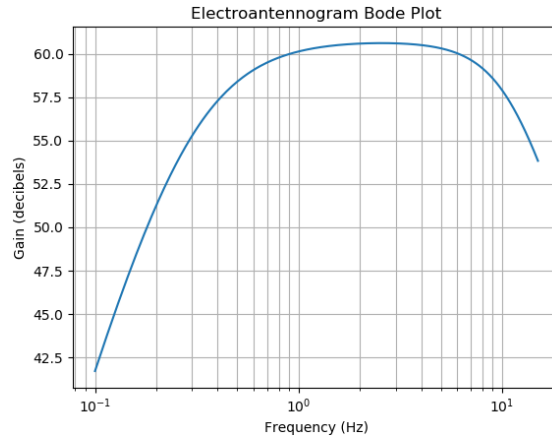


Figure 1.4: EAG model magnitude response

antenna from a *Manduca sexta* moth which we connect to the EAG by inserting a segment of 75 μm diameter stainless steel wire into each end of the antenna.

Rather than use a generic amplifier, our EAG circuit is tuned to the characteristics of antenna from *Manduca sexta* to provide a low noise and high amplitude output signal. We found our antenna preparation will produce a voltage signal between 10 μV and 1 mV in response to chemical stimuli, so we fixed the gain of the EAG to 1000. The antenna signal also contains an undesirable offset voltage that drifts over time in a manner unrelated to the chemical stimulus, causing a previously noted baseline drift [3]. Lastly, we found that the resistance of our antenna preparations ranges from 500 to 750 $\text{k}\Omega$. The large resistance of the antenna preparation causes 60 Hz noise from the environment to appear at the input. To attenuate this 60 Hz noise, and remove the effect of baseline drift on the EAG output, our design includes a 4th order bandpass filter. The magnitude response of the EAG model is shown in Fig. 1.4.

Due to the large gain of the circuit, we observed that the total input offset voltage of the preamplifier can cause the output signal to saturate, and thereby corrupt the chemical signal. To reduce the total input offset voltage error, we used INA118 from Texas Instruments for our preamplifier because it features 1 nanoamp input offset current and 20 mV input offset voltage. As a result, our EAG design rejects baseline drift at the output, can tolerate 10 mV

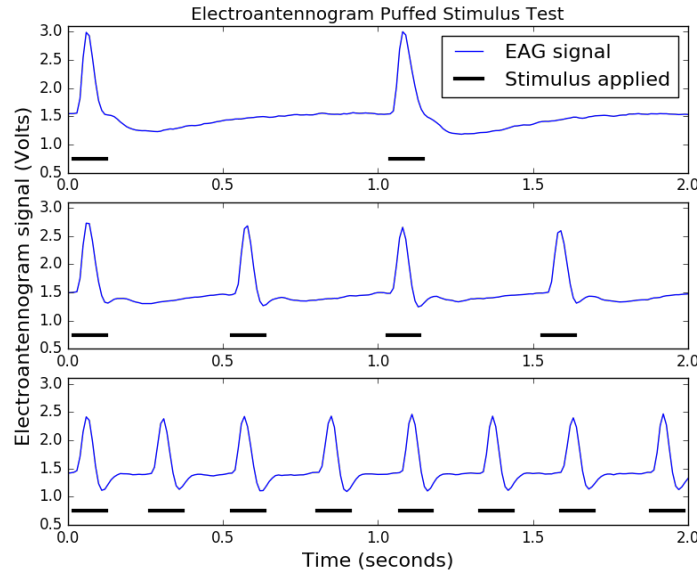


Figure 1.5: The EAG response to a hand puffed stimulus. Floral scent is hand puffed using a disposable pipette perpendicular to the intake of a mini wind tunnel containing the EAG.

of offset voltage without affecting the output signal, and attenuates high frequency noise to provide a high signal to noise ratio.

We validated the EAG design by stimulating the antenna excised from a cold anesthetized moth with a floral mixture of compounds present in the flower *Datura wrightii* [8] which the *Manduca sexta* moth feeds from. This mixture is an attractant for both female and male *Manduca sexta* and is effective in producing EAG responses. The composition of this mixture is shown in Table 1.1.

We deposited 5 μL of the scent mixture on the inside of a disposable pipette and allowed it to dry. This way, when the pipette is squeezed it expels a puff of floral scented air. The EAG was placed inside of an OMEGA mini wind tunnel with airspeed at 2.5 m s^{-1} . The pipette is placed perpendicular to the air flow at the intake of the wind tunnel to ensure that the antennal response recorded is due to chemical stimulus and not to mechanical stimulus from the puffed air. The pipette is puffed by hand at various frequencies. Each stimulus results in an obvious spike in the output signal that decays in a fraction of a second.

Compound	Concentration (mL)
Benzaldehyde	0.02
Benzyl Alcohol	0.5
Geraniol	2
Linalool	0.05
Mineral oil (dilutant)	2.5

Table 1.1: Chemical composition of floral scent.

Fig. 1.5 shows the signal recorded from the EAG when stimulated with scented air. In the plots, the stimulus was delivered by hand at approximately 1, 2, and 4 Hz with the aid of a metronome. The black bars in each subplot are approximations which represent the onset of the stimulus. In contrast to metal oxide sensors, the response and recovery times of antennal EAGs are quite rapid, under a quarter of a second.

1.2.B Nanodrone System Architecture

The EAG sensor interfaces with an autonomous nanodrone. For this, we used a commercially available nanodrone called Crazyflie 2.0 that features open source software and extensible open hardware. The Crazyflie occupies just 85 cm² and weighs only 23 g, placing Crazyflie among the smallest autonomous nanodrones on the market. In addition to the stock Crazyflie, we have added to it an external sensor that is designed by the manufacturer. This sensor uses an optical flow camera and infrared laser range finder to provide the Crazyflie with velocity measurements, which allows the Crazyflie to hover without drifting and without a GPS system. When carrying this payload, the Crazyflie can fly for up to seven minutes from a single cell lithium-polymer battery with 250 mAh of capacity. The Crazyflie also includes a Bluetooth radio transceiver, and the manufacturer sells a USB radio dongle for which a python driver library is available so that users can access vehicle telemetry and controls from an external computer.

Using the radio dongle, our implementation retrieves the EAG data and state information

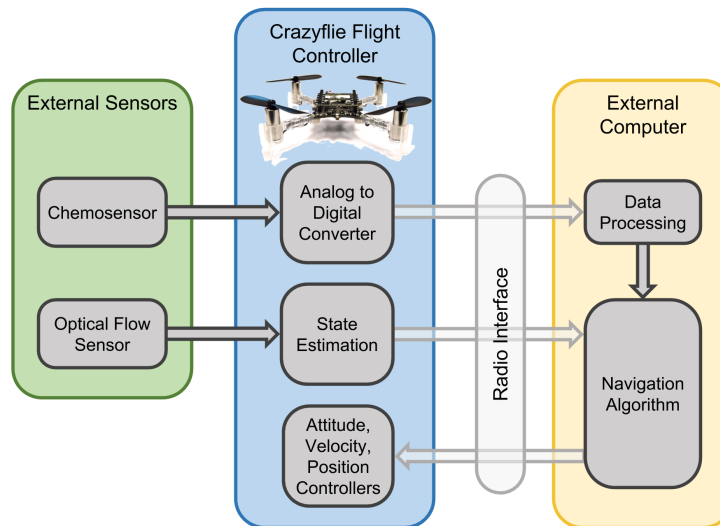


Figure 1.6: System architecture diagram

from the Crazyflie and inputs the data into a navigation program. This program then uses the radio dongle to send velocity commands back to the Crazyflie. Similarly to Luo et al [2], we used an external computer run the navigation program; however, our navigation program consists only of simple thresholding of the EAG signal and transmitting velocity commands. The Crazyflie is fully capable of running the program with no additional hardware. We only used an external computer for its ease of use in programming and debugging. An overview of the architecture of the entire system is presented in Fig. 1.6.

1.2.C Navigation Program

To demonstrate an olfactory search using the Smellicopter, we implemented a navigation program similar to one used in [1] that is inspired by the insect foraging in a single horizontal plane. Flying odor tracking insects will often fly in a crosswind casting pattern and encountering an odor will cause the insect to steer into the wind [6]. This crosswind casting can be in the form of spiraling [3], [7], zigzagging [7], [9], or simple crosswind back-and-forth movement with no upwind component [9]. Although insects perform a three-dimensional

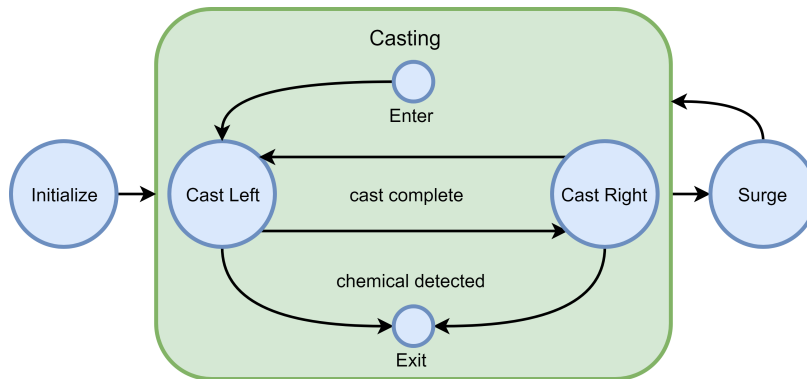


Figure 1.7: Cast and surge state machine.

tracking while following an odor plume, 3D algorithms have not been tested on flying platforms yet. Luo et al [2] does locate a source in 3D but uses a multistage approach which consists of a separate vertical search algorithm to find the altitude of a turbulent plume and then switches to a horizontal only search algorithm to locate the source. Our implementation, illustrated in Fig. 1.7, uses a zigzagging strategy, and it requires that the Smellicopter is in an environment with a relatively consistent wind or airflow. We chose to focus on testing an existing strategy that has been extensively tested in literature, the 2D cast-and-surge algorithm, to show our bio-hybrid platform’s odor localization capability. Future work will test other localization strategies including casting in a vertical direction in addition to crosswind casting.

For our 2D cast-and-surge tests, the vehicle takes off to a height of 40 cm and then hovers for ten seconds to allow it time to orient upwind. The Smellicopter starts casting left and right crosswind. When a volatile chemical is detected, the Smellicopter will surge 25 cm upwind, and then resume casting. Volatile chemicals are detected by simple thresholding of the EAG signal. As long as the wind direction is fairly consistent, this strategy will bring the insect or robot increasingly closer to a singular source with each surge. Moreover, the casting allows the insect or robot to regain the plume even if there is a slight shift in the wind direction or movement of the source; however, the algorithm requires that the Smellicopter is facing upwind most of the time.

1.2.D Upwind Flying

Knowing the wind direction is an important capability for performing an olfactory search because it allows the robot to narrow the set of search directions. Past efforts to perform olfactory search using autonomous UAVs have used numerical methods to estimate the wind vector. Neumann et al used the law of cosines to compute the wind vector from the wind triangle [1], but that required an airspeed reference function that was derived from wind tunnel characterization of the drone. Luo et al estimated the direction of the wind by filtering the UAV attitude [2], but this method requires that the wind speed imparts an attitude bias that exceeds the uncertainty of the attitude state estimate.

In contrast, we have used a passive control scheme to force the Smellicopter to constantly face upwind by adding thin plastic wind vanes to the back motor mounts and modifying its yaw controller. The internal yaw PID controller of the Smellicopter is disabled, and the gains of the yaw rate controller are reduced. The wind vanes are oriented such that if the Smellicopter is not facing upwind, the force of the air flow on the vanes imparts a large yaw torque, causing the Smellicopter to rotate until it is facing upwind. This process works much like a weather vane, where the wind force on the tail of the vane rotates until the weather vane is facing upwind. The Smellicopter holds its position using optic flow while allowing the wind force on the wind vanes attached to the back to rotate the whole vehicle until it is facing upwind.

1.3 Demonstration

To demonstrate the ability of the Smellicopter to localize a chemical source, we designed a simple olfactory search task. We placed a filter paper disk with floral scent deposited on it at intake of a wind tunnel that is 2 m long with a 1 m square cross-section. We set the wind speed at approximately 1 to 1.5 m s⁻¹. We started the Smellicopter at varied positions near the output of the wind tunnel and had it perform the cast and surge algorithm illustrated in Fig. 1.7.

The source is a 2 cm diameter circle of filter paper with approximately 5 mL of floral scent defined in section 1.2.A above deposited on it immediately before beginning the trial.

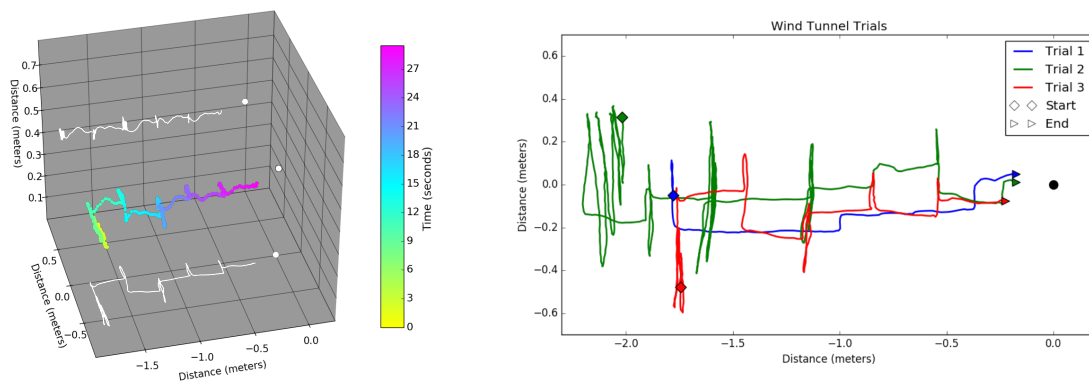


Figure 1.8: Tests of the Smellicopter performing an olfactory search in a wind tunnel, where the wind direction is from right to left. On the left is a single test colored to show time duration and with vertical and horizontal projections of the flight path. A top-down projection of the same test and two additional trials with varied starting positions are shown in the right plot. The position of the source is marked with a circle in each plot.

When using a newly excised antenna from a cold anesthetized moth, the Smellicopter was first hovered both in the presence of odor and in the absence of odor to manually tune the threshold value of the electroantennogram so that any electrical or mechanical noise is rejected and only signals resulting from odor response pass the threshold. Chemical sources used in odor localization experiments with electroantennograms commonly use higher concentrations than are naturally occurring to ensure activation of the antenna within the plume. We chose this amount and concentration of floral scent to show that our platform can successfully follow a chemical plume to its source. Future experiments will test varying odor concentrations.

The left plot in Fig. 1.8 shows the Smellicopter navigating to the source of the odor plume. Multi colored line shows the 3D trajectory of the Smellicopter as estimated from its optic flow-based position estimator. White lines show the vertical and horizontal projections of the 3D trajectory and white circles show the location of the source relative to each path. The colorbar indicates the time progression of the trial, which was approximately 30 seconds. The wind tunnel is as described in the Experimental Setup above with the wind direction

from right to left. The Smellicopter's position is estimated from the optical flow data and verified using video.

This test and two additional tests are shown in the right plot of Fig 1.8 in a top-down view. The Smellicopter starts on the ground downwind of the source in varied locations. The Smellicopter takes off and hovers at a height of 40 cm above the platform and hovers in place for 10 seconds while the yaw control is lowered to allow passive upwind orientation as was described in section 1.2.D. If the Smellicopter detects an odor, it surges upwind. While the Smellicopter does not detect an odor, it casts crosswind with increasing casting width. The tests are automatically terminated once it is approximately 10 cm downwind of the source to avoid the Smellicopter colliding with the intake screen of the wind tunnel.

Our tests show that the Smellicopter rapidly approaches the source, and in each test the Smellicopter ends its search algorithm within 3 cm of the source in the y axis. Each trial ends approximately 10 cm from the source in the x axis to avoid collision with the intake grate of the wind tunnel. The navigation program we demonstrated does not yet have the capability of identifying the source. With the current search strategy if the trial was not terminated and the intake grate did not impede the motion of the Smellicopter, the final surge would move the Smellicopter past the source. At this point, it would be upwind of the source and stay in the casting state. In this situation it would continue to cast until a chemical signature from a new source is acquired, or until the wind direction shifts so that the Smellicopter is downwind of the source once again.

1.4 Conclusion

A biological chemical gas sensor was developed and integrated on a nanodrone where a biologically inspired cast and surge algorithm was used to successfully localize a chemical gas source in a hardware demonstration. To the authors' knowledge, the work reported here represents the first time a biological odor detector has flown on an aerial robot and a passive method has been used to determine wind direction; furthermore, this work is the first to demonstrate such an aircraft operating with sensor autonomy, that is, relying on no external position information while still improving vehicle speed and processing requirements over prior work.

1.4.A Future Work

The Smellicopter is a unique platform that has great potential to be used to test biological hypothesis for insect flight or as a tool to help save lives by finding survivors in disaster areas and detecting hazardous chemical leaks.

Recent advances in genetic engineering and the development of the gene editing tool CRISPR allow for the electroantennogram to be sensitive to additional chemicals other than the molecules that the antennae are naturally sensitive to. In particular, the genome of the *Manduca sexta* moth has been fully sequenced which will allow our current electroantennogram circuitry to detect signals from an antenna with genetically edited odor binding proteins. With this capability, the Smellicopter can use multiple antenna to detect and discriminate between odors that the moth is naturally attracted to as well as detect chemicals such as explosives and people for search and rescue.

The Smellicopter has potential for more realistic physical demonstrations of various odor localization approaches than what is possible in models. Chemical plumes and dynamic wind conditions are challenging to model, especially when combined with vehicle dynamics and control. The Smellicopter is a robust, affordable platform which would allow rapid testing of olfactory search strategies in hardware and under realistic conditions. Additionally, because the Smellicopter is similar in size to insects such as the *Manduca sexta*, and the electroantennogram does not have the latency of commercial sensors, it is an ideal platform for comparing bio-inspired odor localization strategies. One such example is to investigate whether insects search behaviors are purely reactive or whether they maintain an internal model of the plume to optimize their search trajectory [10], [11]. Due to the power and weight constraints of drone platforms, determining the optimal search strategy given a unique task, such as locating trapped persons or a hazardous chemical leak, is vital to the timely success of the completing the task. Using the Smellicopter as a platform to test these strategies and optimize them will bring us one step closer to making life-saving drones reality.

ACKNOWLEDGMENT

This work has been funded by grant FA9550-14-1-0398 from the AFOSR, by the Komen Endowed Chair to TLD, and by the National Defense Science and Engineering Graduate Fellowship. We also thank the Dr. Timmer Horiuchi for suggesting wind vanes, the AFRL Scholars program, and members of the Daniel and Fuller labs at the University of Washington.

Chapter 2

A BIO-HYBRID ODOR-GUIDED AUTONOMOUS PALM-SIZED AIR VEHICLE

Melanie J Anderson¹, Joseph G Sullivan², Timothy K Horiuchi³, Sawyer B Fuller¹⁴, and
Thomas L Daniel¹⁵

Chapter 2 is a publication in the peer-reviewed journal *Bioinspiration & Biomimetics* by IOP Publishing on December 16, 2020.

The main contributions of this work are 1) showing comparisons of the refined electroantennogram sensor vs commercially available odor sensors, 2) demonstrating repeatable autonomous odor localization of the whole system in a wind tunnel environment, 3) demonstrating obstacle avoidance during odor localization.

¹University of Washington, Department of Mechanical Engineering, Seattle WA 98195, USA

²University of Washington, Department of Electrical and Computer Engineering, Seattle WA 98195, USA

³University of Maryland, Department of Electrical and Computer Engineering, College Park MD 20742, USA

⁴University of Washington, Paul G. Allen School of Computer Science, Seattle WA 98195, USA

⁵University of Washington, Department of Biology, Seattle WA 98195, USA

Abstract

Biohybrid systems integrate living materials with synthetic devices, exploiting their respective advantages to solve challenging engineering problems. One challenge of critical importance to society is detecting and localizing airborne volatile chemicals. Many flying animals depend their ability to detect and locate the source of aerial chemical plumes for finding mates and food sources. A robot with comparable capability could reduce human hazard and drastically improve performance on tasks such as locating disaster survivors, hazardous gas leaks, incipient fires, or explosives. Three advances are needed before they can rival their biological counterparts: (1) a chemical sensor with a much faster response time that nevertheless satisfies the size, weight, and power constraints of flight, (2) a design, sensor suite, and control system that allows it to move toward the source of a plume fully autonomously while navigating obstacles, and (3) the ability to detect the plume with high specificity and sensitivity among the assortment of chemicals that invariably exist in the air. Here we address the first two, introducing a human-safe palm-sized air vehicle equipped with the odor-sensing antenna of an insect, the first odor-sensing biohybrid robot system to fly. Using this sensor along with a suite of additional navigational sensors, as well as passive wind fins, our robot orients upwind and navigates autonomously toward the source of airborne plumes. Our robot is the first flying biohybrid system to successfully perform odor localization in a confined space, and it is able to do so while detecting and avoiding obstacles in its flight path. We show that insect antennae respond more quickly than metal oxide gas sensors, enabling odor localization at an improved speed over previous flying robots. By using the insect antennae, we anticipate a feasible path toward improved chemical specificity and sensitivity by leveraging recent advances in gene editing.

2.1 Introduction

Enabled by revolutionary advances in genetic engineering, artificial intelligence, and ubiquitous computing, there has been an explosion of research integrating living and synthetic systems. From robotic prostheses for amputees [12], to implantable deep brain stimulation chips [13], to reprogrammed cellular organisms [14], such biohybrid technologies have yielded

breakthroughs in problems at the intersection of biology and engineering. In addition to the deployment of devices into living systems, the complimentary arrangement of integrated living structures into robotic devices—biohybrid robotics—is an emerging technology. Examples of this include utilizing biological cells and tissues as living actuators in artificial machines [15], or creating a biohybrid robot from a living system, such as a jellyfish, by embedding control electronics [16]. In Biohybrid Robotics, living systems are exploited to exceed what is possible in strictly man-made systems.

2.1.1 Odor localization

Robotic odor localization in natural and artificial environments is an open challenge of critical importance in life-saving applications. A robot with appropriate chemical sensing capabilities could be used to locate trapped survivors in a disaster, to search for leaks of hazardous chemicals in industrial settings, or to locate explosives or chemical warfare agents in conflict zones. These tasks are well suited to robots because they pose substantial risk to humans or canines. In addition, odor localizing robots could reduce the work of first responders in a disaster by allowing fewer people to search larger areas for survivors. Despite ample research interest and motivation for odor localizing robots, the limited odor sensing performance and stringent size, weight, and power (SWaP) constraints of small robots have hampered their widespread use for such applications.

In contrast, chemical sensing is a universal capability of living organisms across all scales and taxa. Most animals depend on this ability for their survival. Combined with a suitable search strategy, animals can use chemosensing to find the source of chemical emissions which may come from potential mates or food sources [4]. Moreover, flying animals have evolved sophisticated sensing capabilities and olfactory search behaviors that allow them to efficiently search in highly complex 3D environments such as the forest canopy, which include myriad obstacles and turbulent flow. For example, male moths can track females over great distances, detecting female pheromones at concentrations far less than parts per trillion [5]. Female mosquitos use a sense of carbon dioxide to find food [17], and fruit flies sense ethanol [18].

A distinguishing characteristic of plume tracking by animals is the use of near- instantaneous information present in the plume [4, 19]. Plumes in the air typically consist of a patchy distribution of filaments containing high chemical concentration interspersed among large areas of low concentration. This is because convection dominates over diffusion for transport in atmospheric flow, which is turbulent [4].

2.1.2 Flying smelling robots

Recent research has strived to approach the remarkable odor search capability of living systems using robots. Flying robots are well suited to this task as they can search for odor sources at various altitudes, avoid difficult terrain, and manage obstacles without sophisticated ambulatory systems. Important advances in plume source localization with flying robots include a 1 m multi-rotor drone that follows an outdoor methane plume to its source in two-dimensional space [1]. This drone used semiconductor metal oxide (MOX) sensors, which have low chemical specificity, a slow rise time and long recovery period in the presence of high gas concentrations [3, 20]. To achieve reliable readings, the drone must pause at each sampling location for 20 seconds for the sensor to stabilize, necessitating a search time lasting tens of minutes, nearly as long as the drone's battery life. In another recent work, Luo et al [2] showed that with improved signal processing, an array of MOX sensors could extract odor information from a plume on a short timescale. However, their signal processing algorithm is computationally intensive, and requires constant communication to an offboard computer with a powerful GPU. Burgúes et al [21] has achieved odor localization in a multi-room space using a calibrated MOX to sense an indoor chemical source on a palm-sized drone. They were able to consistently locate odor sources, but their approach relied an external absolute positioning system, a map of the room, and repeated traverses, which are not typically available in environments of practical interest. Shigaki et al implement a moth-inspired strategy on a pocket-sized drone using MOX sensors [20]. They apply an inverse sensor model in order to improve the signal from the MOX sensors and are able to successfully fly toward an alcohol source over a 2 meter distance. Other work on source localization has investigated different sources such as light which allows a gradient

search unaffected by wind. One example of this shows that a small drone platform carrying a light sensor can use a deep reinforcement learning policy to find the source of a light even in the presence of obstacles [22]. Hence the state of the art continues to be challenged by the speed and reliability of suitably small synthetic chemical sensors and size-constrained navigation systems.

2.1.3 Electroantennograms (EAGs) and natural chemical sensing

Biological odor detectors, such as moth antennae, outperform state-of-the-art (engineered) portable chemical sensors in detection speed, sensitivity, and chemical selectivity. The extreme sensitivity and rapid response times of natural chemical sensing arises, in part, from an energy dependent G protein-coupled amplification system that can convert single molecule detections into electrical signals in odor-detecting neurons of the moth antennae [23]. These electrical signals, known as EAG, can be measured using highly sensitive amplifiers. While moths discriminate between odors by sensing signals from individual neurons, EAGs are the combined response of all the neurons.

Use of EAGs coupled to the antennae of moths has been previously demonstrated on mobile robots for chemical plume tracking. Notable examples of biohybrid robotic systems using living sensors on ground robots include a mobile robot in a wind tunnel using a moth EAG [24], an odor tracking mobile robot steered based on input from a moth's ambulation motions on a sensitive trackball [25], and a ground robot capable of avoiding collisions by using a fly's visual system to perform optic flow estimates [26]. There have also been some systems integrating biological and bioinspired components on flying systems such as a drone being steered by an off-board moth on a trackball [20] and the development of an algorithm to improve an EAG signal onboard a tethered 0.5 meter drone [27].

2.1.4 The "Smellicopter": a biohybrid system

In this work, we introduce the use of an insect's chemosensory apparatus on a flying robot dubbed the 'Smellicopter'. By doing so, we leverage the sophisticated and fast G-protein-mediated chemosensing capabilities that have evolved in biology to provide a sensor with

a speed that better matches rapid motions possible with flight. Our EAG-based system uses antennae from the hawkmoth *M. sexta* for a lightweight (1.5 g) and extremely low-power (2.7 mW) sensor. We show that it has a much faster response than MOX sensors, and deploy it on a small, palm-sized 30 g hovering four-rotor aircraft. We then equipped this biohybrid system with a sensor suite that allowed it to control its position and avoid obstacles while moving through confined spaces fully autonomously. To enable the robot to navigate a chemical plume, we additionally introduced wind fins fixed to the robot, which cause it to passively orient into the wind. This allows for a simple, reactive search that relies on the robot operating in a coordinate system rotated to a wind-oriented reference frame at all times. In previous work [28], we presented a proof of concept for this system. Here, we expanded its capabilities to include operation in confined spaces with obstacles and provide a more detailed analysis of EAG and robot system performance. We show that our biohybrid robot navigates to the source of an airborne odor plume in a confined wind tunnel repeatedly over 15 independent trials, and uses laser ranged distance estimates to avoid obstacles. Our robot uses a bioinspired cast-and-surge strategy, without any need for external position information such as from the global positioning system (GPS).

The aggregation of these advances represents a significant advance in robotic plume source localization because with them we are able to, for the first time, quickly and fully autonomously, navigate to a chemical plume source in an environment including obstacles as would be encountered in many real-world applications. Furthermore, we anticipate that our biological sensor has the potential for designing chemical specificity using recent advances in genetic engineering to express chemical-specific chemosensors [29].

2.2 *Design and system architecture*

2.2.1 Structure and control architecture

Our palm-sized air vehicle, the Smellicopter (figure 2.1(a)), is built from a commercially available quadcopter, the Crazyflie 2.0 (Bitcraze AB). We use two additional commercial sensor decks that have functions critical for autonomy: the flow deck (Bitcraze AB) which has down-facing optical-flow and range sensors and the multi-ranger deck (Bitcraze AB)

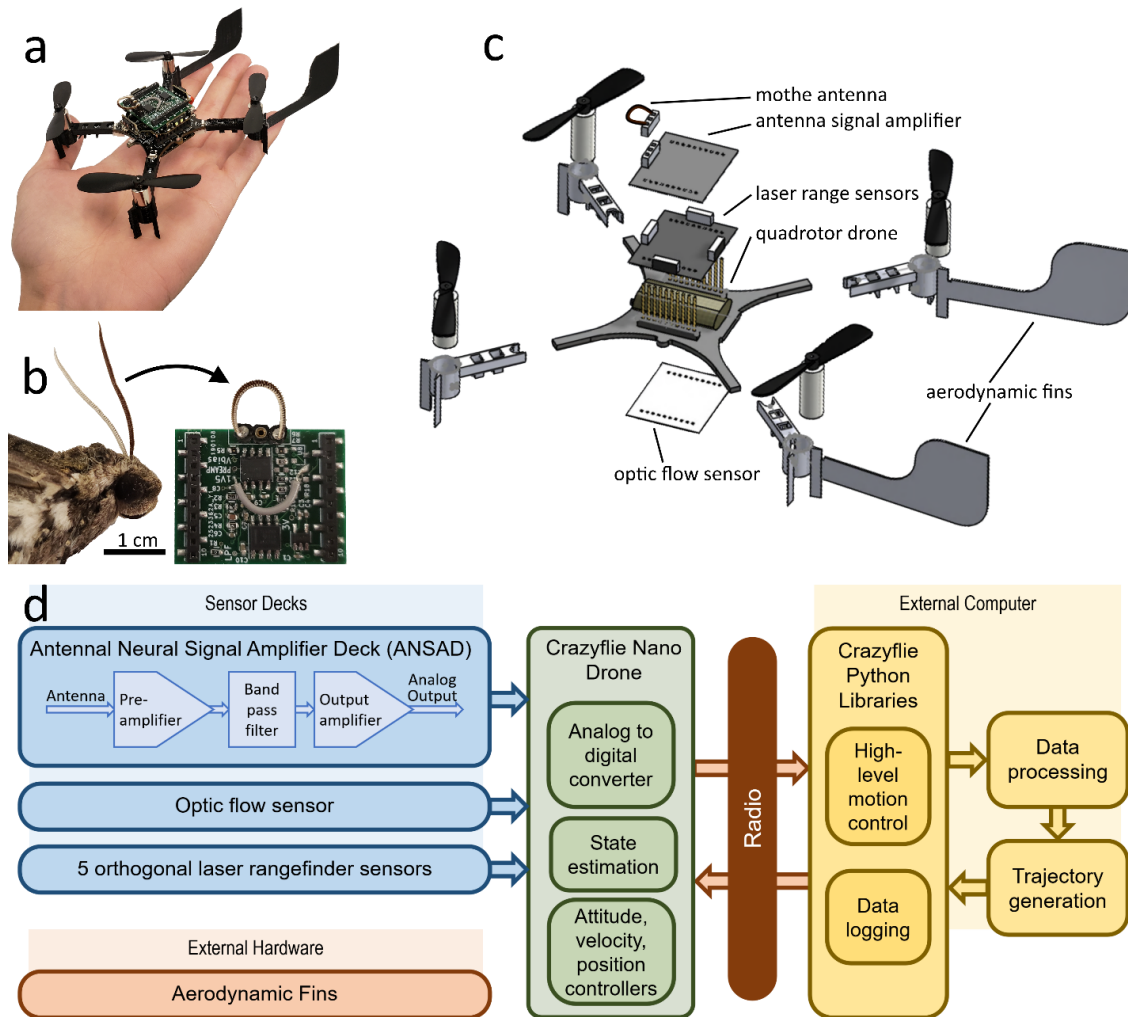


Figure 2.1: Anatomy and control architecture of the ‘Smellicopter’. (a) A photo of the Smellicopter in a hand. (b) A closer view of the antennal signal amplifier deck next to the head of a *M. sexta* moth. (c) A disassembled view of the Smellicopter. (d) An overview of the system architecture.

which has five-directional range sensing. The optical-flow sensor provides body-frame velocity measurements that allow the quadcopter to hover in-place indoors without GPS or a motion capture camera system. The laser range sensors provide range measurements in four directions in the horizontal plane (forward, back, left, right), allowing the quadcopter

to detect and navigate around obstacles. In addition to the commercial components, we have added two custom innovations: our antennal neural signal amplifier deck (ANSAD) (figure 2.1(b)) and the aerodynamic fins. The ANSAD generates an EAG providing the Smellicopter with odor information. The aerodynamic fins passively steer the platform upwind to perform the odor localization algorithm. The component configuration is shown in figure 2.1(c).

The Crazyflie, built from extensible open hardware, occupies just 85 cm² and weighs only 23 g, placing it among the smallest autonomous air vehicles on the market and making it ideal for indoor use. When carrying the additional components, the Crazyflie can fly for up to 7 min from a single cell lithium–polymer battery with 250 mAh of capacity.

Our platform communicates over a 1 Mbyte/s bluetooth radio link, receiving EAG data, range information, and state information from the Crazyflie, which is provided to a navigation program (figure 2.1(d)). This program then uses the radio to send velocity commands back to the Crazyflie. Like Luo et al [2], we used an external computer to run the simple navigation program. However, our program has minimal computational requirements and can be fully implemented within the 32 bit microcontroller on the Crazyflie. In this work we use an external computer solely to simplify the workflow of implementing and testing the navigation program.

2.2.2 On-board electroantennograms (EAGs) and metal oxide (MOX) sensors

Antennae serve as critical sensory organs for insects and other arthropods. In addition to their capacity to sense wind [30] and vibrations [31], antennae most notably provide olfactory information to the insect to find food and mates [6]. Chemical sensing follows from a complex cascade of molecular interactions [23]. Volatile compounds diffuse into the interior of the antenna where they then bind to odor-binding proteins. Those complexes then bind to, and activate, G-protein receptor molecules on the membranes of chemosensory neurons populating the interior of the antenna. Once activated, G-protein-mediated pathways provide a whole cell response that greatly amplifies the influence of a single odorant molecule. That amplified response yields, in turn, an action potential that propagates down the an-

tennal neuron to the brain of the insect. With thousands of olfactory neurons in an antenna [32], an EAG represents their aggregate electrical activity by the voltage drop across the length of the antenna. An EAG therefore provides an electrical reading of a neural process, much as is done for electromyograms (EMG) or electroencephalograms (EEG).

The ANSAD circuit, which produces the EAG, consists of three cascaded filtering and amplification stages that are tuned to the responses in antennae from *M. sexta*, resulting in a low-noise, highly amplified EAG signal. The ANSAD weighs 1.5 g and consumes only 2.7 mW, imposing minimal weight and power requirements on the platform [28]. The ANSAD circuit board is designed to mount directly onto the Crazyflie drone platform in the same manner as the other commercial add-on decks. The antenna is oriented toward the front of the drone, where the flow from the rotors will pull air over the antenna. This downwash is suspected to enhance the signal, much like how flapping wings can enhance the flow of air over the antenna of a flying insect, thereby increasing the amount of air which can be sampled for odors [33].

Antennae isolated from cold anesthetized *M. sexta* moths were connected to the ANSAD via 75 μm diameter stainless steel electrodes. This preparation results in an EAG that responds to particular volatile chemicals rapidly, with a maximum bandwidth of 10 Hz [3], providing the capability to make multiple chemical detections in quick succession. We tested the EAG sensor by stimulating the antenna with the custom floral mixture presented in [28], comprised of compounds present in the flower *D. wrightii* [34], a common floral nectar source for *M. sexta*. This mixture is an attractant for both female and male moths and is effective in producing EAG responses. These antennae continued to produce signals for at least 2 h and up to 4 h. The signal strength, however, continuously declines over this period as has been noted in other insect species [3]. The lifespan of the severed antenna is still many times the flight time of a drone and can be used for multiple successive trials.

We tested the performance of the ANSAD and compared it to a similarly sized commercial MOX sensor, the MiCS-5524, which consumes approximately 150 mW and is nearly identical to the sensors used in other odor localization work [20, 2]. We deposited 5 μl of the scent mixture and 10 μl of 50% ethanol on a 1 cm diameter filter paper placed inside of a disposable pipette. When the pipette is squeezed it expels a puff of floral and ethanol

scented air. The EAG and MOX sensors were placed adjacent to one another inside of an OMEGA mini wind tunnel with airspeed at 2.5 m s^{-1} . The MOX sensor is facing toward to upwind direction and the EAG sensor is placed in the upright position same as if it were mounted on the drone. The pipette is placed perpendicular to the air flow at the intake of the wind tunnel to ensure that the antennal response recorded is due to chemical stimulus and not to mechanical stimulus from the puffed air. The pipette is puffed by hand at various frequencies. Each stimulus results in an obvious spike in the output signal that decays in a fraction of a second. We quantified the rise and fall times by computing the time between 10 percent of the peak value to the time of the peak value and from the time of the peak value to 10 percent of the peak value respectively.

2.2.3 Cast-and-surge localization with passive fins

The Smellicopter implements an olfactory search using a navigation algorithm that is inspired by the insect foraging in a single horizontal plane [1] (see supplemental video) . Flying odor-tracking insects will often fly in a crosswind casting pattern, and upon encountering an odor, the insect will steer into the wind [6]. This crosswind casting can be in the form of spiraling/looping [3, 20, 7], zigzagging [20, 7, 9], or simple back-and-forth crosswind movement with no upwind component [9]. Although insects perform three-dimensional tracking while following odor plumes, 3D algorithms have not yet been implemented on flying platforms. Luo et al [2] does locate a source in 3D but uses a multi-stage approach which consists of a separate vertical search algorithm to find the altitude of a turbulent plume and then switching to a horizontal only search algorithm to locate the source. Our implementation (figure 2.1(d)) uses a crosswind casting strategy, and it requires that the Smellicopter is in an environment with relatively consistent wind or airflow. We chose to focus on deploying a 2D cast-and-surge algorithm (figure 2.2), which is similar to the existing casting and surging strategies that have been extensively tested in the literature mentioned above.

Crosswind casting demands that the system has wind orientation capabilities. Past efforts to perform olfactory search using autonomous UAVs have used numerical methods to actively estimate the wind vector. Neumann et al [1] used the law of cosines to compute

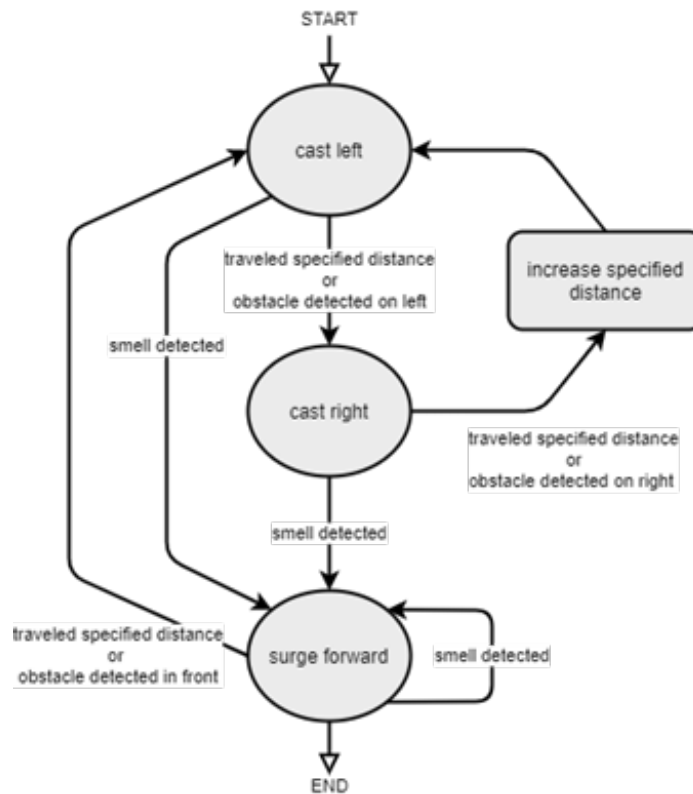


Figure 2.2: Flow chart of the cast-and-surge algorithm. The algorithm begins with casting left for a specified distance and then casting right for that same distance. For each successive cast left and right, the casting envelope distance is increased. If a smell is detected at any time during this process, the algorithm switches to upwind surging for a specified distance. If another smell is encountered during a surge, the surge will continue. If the Smellicopter has surged for the specified distance and has not encountered another smell, it will switch back to the initial casting left stage and reset the casting distance to the starting amount. Additionally, obstacle avoidance can be added to the strategy. When an obstacle is detected in the direction that the Smellicopter is currently moving, the Smellicopter will jump to the next state in the algorithm. The cast-and-surge algorithm is for finding and following a plume. Source detection is another task which is not yet covered. The algorithm is manually terminated before the Smellicopter collides with the front of the wind tunnel.

the wind vector from the wind triangle, but that approach required an airspeed reference function that was derived from wind tunnel characterization of the drone. Luo et al [2] estimated the direction of the wind by filtering the UAV attitude in response to the wind, but this method requires that the wind speed imparts an attitude bias that exceeds the uncertainty of the attitude state estimate.

In contrast, we have used a passive control scheme to force the Smellicopter to constantly face upwind by adding thin plastic wind vanes to the rear motor mounts and by modifying its yaw controller. The yaw angle controller of the Smellicopter is disabled, and the gain of the yaw rate controller is reduced, which allows exogenous torque disturbances to perturb the Smellicopter's yaw angle. The wind vanes are oriented such that when the Smellicopter is not facing upwind, the force of the wind airflow on the vanes imparts a yaw torque to rotate it into the wind. This process works much like a weather-vane. The Smellicopter holds its translational position using the downward-looking optic flow sensor. This method works well in a steady breeze, which could be encountered in situations such as a mine shaft or in a building with opposing windows open.

Volatile chemicals are detected by simple thresholding of the EAG signal using the following method. Prior to the trials, the Smellicopter is manually hovered in and out of the chemical plume and the threshold is manually inputted into the search algorithm. This is necessary because of small variations between antennae. If the EAG signal exceeds this threshold during flight, a surge is triggered. This strategy will bring the insect or robot increasingly closer to an odor source with each surge. Moreover, the casting allows the insect or robot to relocate the plume even if there is a slight shift in the wind direction or movement of the source; however, the algorithm requires that the Smellicopter is facing upwind most of the time.

2.2.4 Multisensor integration with obstacle avoidance

The Smellicopter is equipped with a MultiRanger deck (Bitcraze AB) that uses four infrared range sensors that permit obstacle detection and thus allows it to navigate around obstacles while performing an odor localization strategy. The fifth range sensor which gives a distance

measurement to obstacles above the Smellicopter is unused. To avoid obstacles, the Smellicopter takes range measurements in four directions, ten times per second. When a range measurement in the direction of the Smellicopter's current heading falls below 20 cm, then the Smellicopter will change direction by advancing to the next state of the cast-and-surge search behavior.

For the odor localization and obstacle avoidance trials, we used a source consisting of a 2 cm filter paper disk with 5 ul of the scent mixture deposited on it. The trials take place in a wind tunnel 2 m long by 1 m wide by 1 m tall with a windspeed of approximately 1 m s⁻¹. The source is placed at the front of the wind tunnel, upwind of the experimental area.

2.3 Results

2.3.1 On-board electroantennograms (EAGs) vs metal oxide sensors

We compared the sensitivity and response of the EAG produced by our sensor to a commercial MOX sensor similar to those used in other odor localization studies [20, 2] (figure 2.3). Our EAG sensor and a metal oxide (MiCS-5524) sensor were tested simultaneously with floral scent and ethanol. Twice as much stimulus (ethanol) was used for the MOX sensor as was used for the EAG sensor (floral scent) to produce a visible signal from the MOX sensor. A digital filter is applied to the MOX sensor signal with the same transfer function as the analog filter in the ANSAD circuit, which has low and high cutoff frequencies at approximately 2 Hz and 60 Hz respectively.

The EAG signal rise time (time from 10% of peak to peak) and fall time (time from peak to 10% of peak) were less than half of that of the MOX signal (table 2.1). The EAG signal has a negative component due to the filtering circuitry. The sensors were placed directly adjacent to one another in the wind tunnel, but due to the size of the sensors, the separation between the sensing portions was around 1.5 cm. This separation and the patchy nature of airborne odor plumes causes the responses from the sensors vary between stimulations.

		<i>Peak height (V)</i>	<i>Rise time (s)</i>	<i>Fall time (s)</i>
<i>EAG</i>	Mean	1.425	0.045	0.045
	Standard deviation	0.098	0.015	0.007
<i>MOX</i>	Mean	0.413	0.104	0.198
	Standard deviation	0.095	0.013	0.021

Table 2.1: EAG vs MOX comparison. Signal rise time is the time from 10% of peak to peak, signal fall time is the time from peak to 10% of peak.

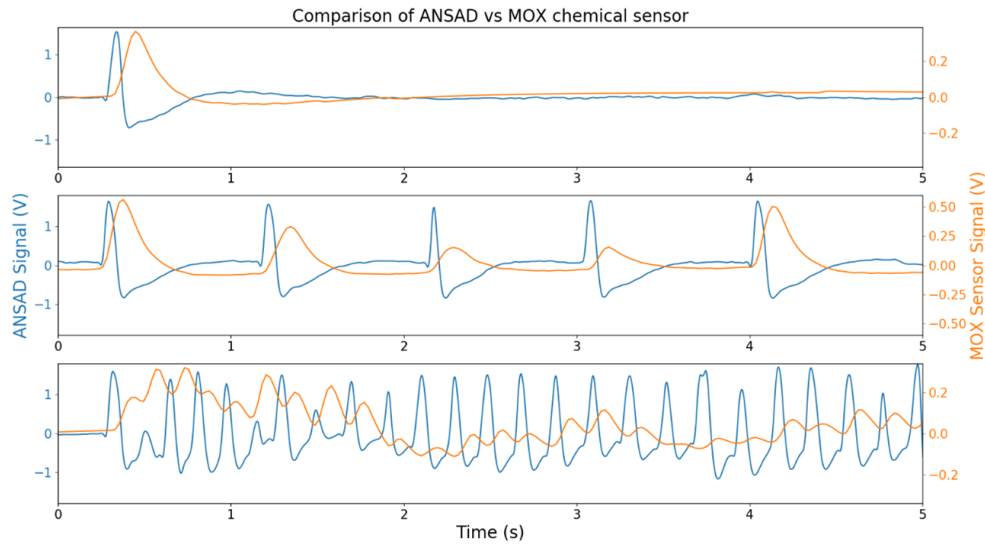


Figure 2.3: EAGs from a moth antenna and signals from metal oxide sensors. Three trials show the time course of signals recorded from the ANSAD sensor and the MOX sensor when stimulated with scented air. 5 μl of custom floral scent [28] and 10 μl of 50% ethanol is deposited on a 1 cm diameter filter paper disk and placed into a disposable pipette. The stimulus is hand puffed perpendicular to the intake of an OMEGA mini wind tunnel with windspeed at 2.5 m s^{-1} . In (a), the stimulus is delivered once. In (b) and (c), the stimulus was delivered by hand at approximately 1 and 5 Hz with the aid of a metronome. Data were recorded at approximately 42 samples per second.

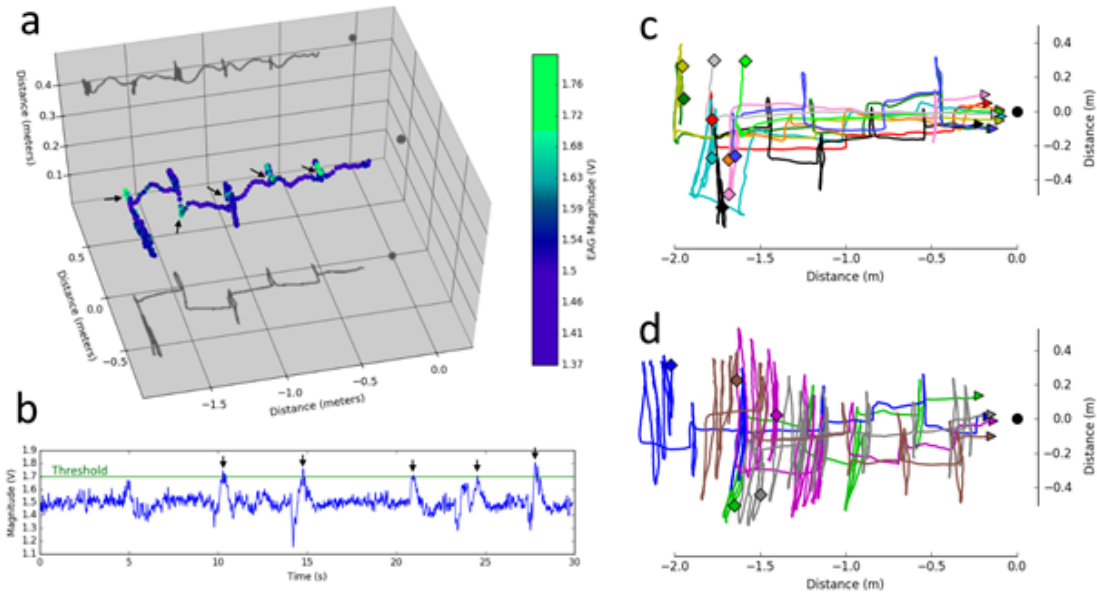


Figure 2.4: Odor localization trials. (a) A single trial of the Smellicopter navigating to the source of the odor plume. Wind speed was estimated to be approximately 1 m s^{-1} . The multicolored line shows the 3D trajectory of the Smellicopter as estimated from its optic flow-based position estimator. Grey lines show the vertical and horizontal projections of the 3D trajectory and grey circles show the location of the source relative to each path. The color bar indicates the voltage level of the signal from the ANSAD as the trial progresses where blue is no odor sensed, light blue is some odor sensed, and green is enough odor sensed to trigger a surge in the behavior. Places where a surge is triggered are identified with black arrows. The test is performed in a wind tunnel with the wind direction from right to left. The Smellicopter's position is estimated from onboard sensors. (b) The EAG signal of the trial shown in (a). Activity that surpasses the threshold triggers a surge in the search strategy and is marked with a black arrow. (c) and (d) Additional tests in a top-down view. Upper plots are trials with a duration of less than 30 s and lower plots are trials with a duration of greater than 30 s.

2.3.2 *Cast-and-surge localization with passive fins*

For our 2D cast-and-surge tests, the Smellicopter took off to a height of 40 cm and then hovered while the yaw control was lowered to allow passive upwind orientation using the aerodynamic fins. It then began left-right crosswind casting with increasing casting amplitude until a volatile chemical was detected via the ANSAD, at which time it surged 25 cm upwind (i.e. forward). In the absence of additional chemical signals, it resumed crosswind casting. The tests were manually terminated once it is approximately 10 cm downwind of the source to avoid the Smellicopter colliding with the intake screen of the wind tunnel. The plots in figure 2.4 show the Smellicopter’s estimate of its position as it flies through the wind tunnel. This estimate is susceptible to drift over time, so each ending distance to the source (table 2.2) is determined by measuring the distance shown through an overhead camera. In 14 out of 15 trials, the Smellicopter ended within 4 cm of the source in the crosswind direction. All trials ended within 6 cm of the source in the crosswind direction. Distance to the source in the direction parallel to the wind direction is not recorded since the trials are stopped before the Smellicopter collides with the intake screen of the wind tunnel.

2.3.3 *Multisensor integration with obstacle avoidance*

To test the obstacle avoidance capability of our platform, we set up cardboard obstacles inside the wind tunnel environment outlined in the previous experiments (figure 2.5(a)). The wind speed was set to approximately 1 m s^{-1} . As above we used a source consisting of a 2 cm filter paper disk with 5 ul of custom scent mixture deposited on it. Trials were manually terminated when the Smellicopter came within approximately 10 cm of the source in the direction parallel to the wind direction to prevent collision with the front of the wind tunnel. The plots in figure 2.5 show the Smellicopter’s estimate of its position as it flies through the wind tunnel. This estimate is susceptible to drift over time, so the ending positions are determined by measuring the distance shown through an overhead camera. The Smellicopter was able to successfully localize the source of the odor while avoiding the obstacles presented. Figure 2.5(b) and 2.5(c) show two successful trials of the Smellicopter

performing odor localization as well as obstacle avoidance. In each trial, the Smellicopter navigated through the obstacles and ended within 4 cm of the source in the crosswind direction.

<i>Trial</i>	<i>Starting position x (m)</i>	<i>Starting position y (m)</i>	<i>Ending distance to source (cm)</i>	<i>Time duration (s)</i>	<i>Length of total path (m)</i>
1	-1.95	0.07	-4.0	23.91	4.27
2	-1.65	-0.51	5.5	73.14	8.12
3	-1.78	-0.05	2.0	12.40	2.27
4	-2.02	0.31	0.5	79.63	14.27
5	-1.78	-0.27	-1.0	45.78	5.36
6	-1.41	0.02	-0.5	85.32	15.60
7	-1.96	0.27	-2.0	17.95	3.33
8	-1.50	-0.44	1.0	93.12	16.98
9	-1.68	-0.28	0.5	12.44	2.24
10	-1.72	-0.56	-3.0	29.88	5.28
11	-1.64	0.22	-4.0	100.47	11.33
12	-1.68	-0.48	4.0	22.03	3.86
13	-1.59	0.30	0.0	15.90	2.14
14	-1.65	-0.26	-4.0	28.01	3.11
15	-1.77	0.30	-0.5	11.16	2.07
Mean	-1.72	-0.09	-0.37	43.41	6.68
StDev.	0.17	0.33	2.83	33.07	5.27

Table 2.2: Summary data for odor localization trials. For 15 trials we monitored the search duration and path length for the Smellicopter flight in a wind tunnel.

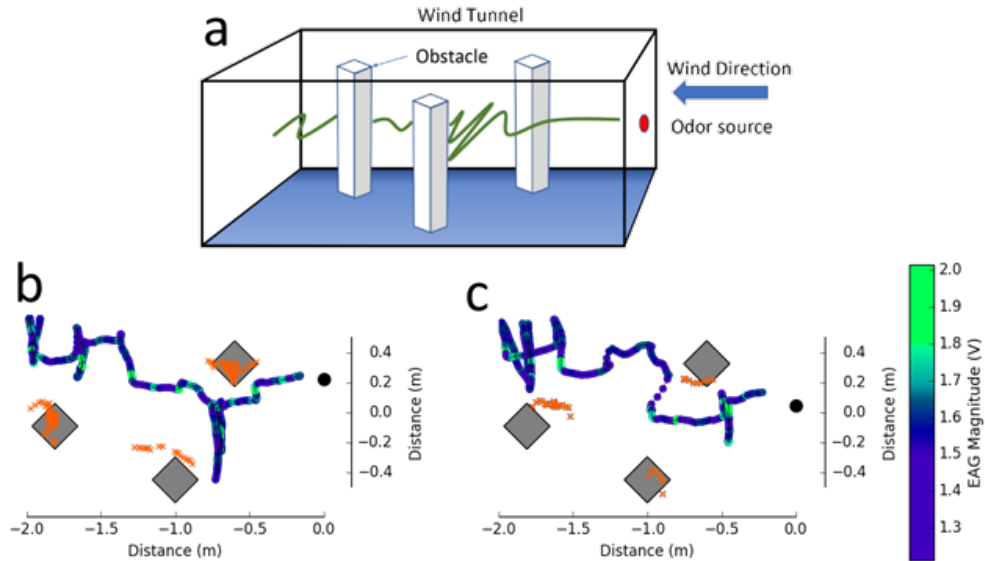


Figure 2.5: Obstacle avoidance trials. (a) A diagram of the obstacle avoidance trial environment. The wind speed is set at approximately 1 m s^{-1} . (b) and (c) Individual obstacle avoidance trials. The blue and green line is trajectory, where blue portions indicate no odor detected, light blue portions indicate increased activity within the EAG signal, and green portions indicate high activity triggering a surge. Grey diamonds are video estimated locations of obstacles. Orange x's indicated range measurements made by the Smellicopter as it is flying past the obstacles. Black circles are source locations estimated by video.

2.4 Discussion

This study has drawn on the synergy between the engineerability of synthetic robotics and the outstanding performance of naturally-occurring sensory systems to create a device that combines the best of both worlds. Thus, we developed a biohybrid flight system capable of autonomously localizing a chemical source via a biologically-inspired plume tracking behavior. It provides a novel solution to a challenging technological problem; one with stringent SWaP constraints. Interestingly, the development of bio-hybrid robotic systems has seen dramatic growth over the last decade, with some systems containing microelectronics embedded into intact living systems [35, 36, 37, 38], devices that contain sensory structures

embedded onto robotic platforms [24, 26, 15], and even robotic platforms with integrated cultured muscle cells as actuators [15]. All these efforts seek to take advantage of the sensor or actuator efficiency of living systems along with the fabrication advantages of artificial systems.

While the integration of natural and synthetic systems presents exciting new horizons for autonomous aerial vehicles, operating under stringent SWaP constraints poses both challenges and opportunities. Indeed, our motivation to turn to natural sensory structures was largely motivated by these constraints. Using the living antennae of moths with electronic amplifiers to generate EAGs is a weight and power efficient way to acquire chemical information, but antennae have a finite lifetime, thus limiting their long-term deployment. That said, the battery life of the Crazyflie is significantly shorter than the longevity of antennae providing EAGs. Typical flight times are constrained to be less than about 10 min for the Crazyflie and our associated additional hardware. In contrast, we were able to maintain stable EAGs for more than 2 h and up to 4 h. Additionally, explanted antennae can be stored on ice for several days prior to deployment on the Smellicopter, suggesting a viable strategy for deployment in locations remote from a laboratory.

Insect antennae respond to hundreds of volatiles [32, 39, 40, 41], providing both a challenge and an opportunity. The insect is able to identify particular chemicals or mixtures by differentiating between the neurons, but our current configuration measures the aggregate electrical activity of the neurons by the voltage drop across the length of the antenna. Our current configuration can function well with any number of volatile cues, but specific responses to a single odorant is challenging if multiple volatiles are present in the plume. Emerging CRISPR technologies, however, may allow gene editing of antennae to target specific volatiles [29]. Future efforts can focus on multiple antennae, each designed for a specific volatile, thus providing detection of more complex chemical signals.

Other limitations related to SWaP constraints include our method for collision avoidance. The current configuration using four side-facing laser range sensors is a lightweight solution to avoid collisions, but works poorly under conditions where the sensor view is tangential to the object or the object is small enough to fit between the detection beams. This limitation could be addressed by adding a sweeping yaw motion to the search algorithm,

but this movement is currently challenging due to our passive upwind orientation. Collision avoidance could also be improved by adding ultra-miniature camera systems, but this would require significant processing for detecting close objects against a visual background and estimating their distance, an approach that could easily exceed the available computational or power resources for small autonomous air vehicles.

Despite these limitations, our biohybrid system holds promise for many applications in which we have used other odor localization solutions, notably the myriad situations in which used dogs have been used to detect and locate drugs, missing people, or volatiles from explosives. Moreover, this aerial robotic system can provide a valuable platform on which we can experimentally explore the complex 3D interaction between aerial propulsion, odor localization strategies, and airflow in the environment.

Supplemental Information

Video of Smellicopter in a wind tunnel with and without obstacles. See Appendix A for files.

Chapter 3

**A POCKET-SIZED BIO-HYBRID CHEMICAL DETECTOR FOR USE
IN RESEARCH, TEACHING, AND INDUSTRY**

Melanie J Anderson*¹, Vikram Iyer*², Joseph G Sullivan³, Mauro Torres⁴,
Sawyer B Fuller¹², and Thomas L Daniel¹⁴

Chapter 3 is a component of a paper which will be submitted to a scientific conference.

The main contributions of this work are 1) showing revised electroantennogram (EAG) circuitry for use with a mobile cellphone, 2) demonstrating the signal decline of a single antenna over time, and 3) comparing the response of our EAG and a metal oxide (MOX) sensor for various chemicals using a custom made automated odor delivery setup.

*first authors

¹University of Washington, Department of Mechanical Engineering, Seattle WA 98195, USA

²University of Washington, Paul G. Allen School of Computer Science, Seattle WA 98195, USA

³University of Washington, Department of Electrical and Computer Engineering, Seattle WA 98195, USA

⁴University of Washington, Department of Biology, Seattle WA 98195, USA

Abstract

Measurement of chemicals and odors has a wide variety of applications ranging from use in agriculture supply chains to detection of hazardous gases, explosives, illegal wildlife, narcotics, and disease detection. Sensing of complex organic molecules required by these applications with extremely small concentrations (parts per trillion) is far beyond the capabilities of even state of the art synthetic sensors. In contrast, natural olfactory systems in animals excel at this task and trained animals like dogs are commonly used for odor sensing. Training and maintaining such animals is however time consuming and expensive, and more importantly does not provide access to the raw sensing data needed to design new sensing systems. In this work, we design a programmable, digital platform that leverages the advantages of natural chemosensory systems. We present SmellPhone, a low cost, miniaturized bio-hybrid sensing platform that measures odors using insect antennae. We develop an end-to-end system including a full amplifier and signal conditioning circuit that reads the electrical signals from a moth antenna and outputs this data to a smartphone. Our design presents an accessible platform for this novel sensing primitive to enable research across a wide variety of application domains. We demonstrate our design works with insect antennae from multiple species for use in pest detection and insect tracking. Additionally we demonstrate its response time and sensitivity dramatically exceed the capabilities of a commercial metal oxide sensor and are sensitive to 6 different food crops to show its potential for sensing in agriculture.

3.1 Introduction

Natural chemical sensory systems have extraordinary capabilities in the rapid and accurate detection of odors. There are myriad examples of natural chemical detection ranging from the ability of dogs to classify individuals who have cancer or covid infections to the ability of flying insects to detect the pheromones of mates at great distances with sensitivities exceeding 1 in 10^{17} . The challenge today lies in melding the outstanding benefits of natural chemical detection with the engineerability of engineered systems. One such example is in the development of small robotic devices that are equipped with harvested chemosensory

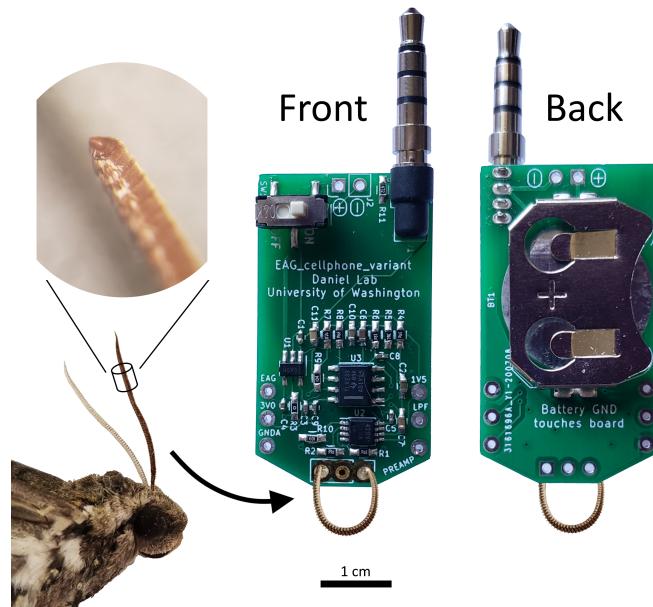


Figure 3.1: The SmellPhone. An antenna from the *Manduca sexta* moth, with cross-section shown, is connected to the SmellPhone circuitry with small wires. The front shows circuitry and audio jack connector and on/off switch. The back shows the coin cell battery holder.

structures from insects. Our recent studies have shown that miniature odor guided systems can localize odor sources through a combining search algorithms on an agile flight platform armed with an intact insect antenna.

Here we present a portable biohybrid chemical sensor which can be used in a variety of situations, such as industry, research, and teaching. The SmellPhone uses custom circuitry to read the neural signals from a moth antenna as it detects chemicals present in the air. The SmellPhone easily interfaces with standard cell phones and a freely available phone application to view and record signals.

The main contributions of this work are 1) the first smartphone connected biohybrid chemical sensing platform, 2) our sensor works with multiple insect species, 3) characterization of odor sensitivity beyond pheromones and flowers, and 4) a custom automated odor delivery system.

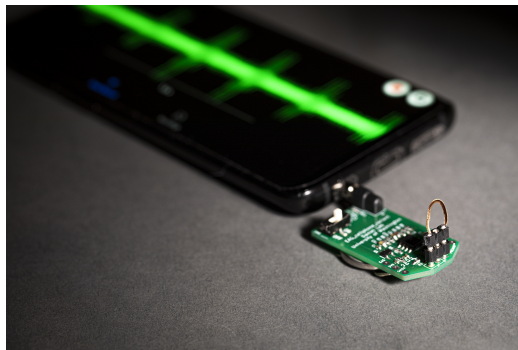


Figure 3.2: The SmellPhone connected to a mobile cell phone showing the antenna signal in real time as it smells odor. Credit = Mark Stone/University of Washington.

3.2 Applications

3.2.1 Food ripening and disease

Agriculture and food supply chains present numerous potential applications for odor sensing. The natural way to determine ripeness of a fruit or to determine if it has gone bad is to smell it. Fruits produce a variety of organic compounds such as phenolics, lipid compounds, esters, terpenes, and many others [42]. The human nose is highly sensitive to a wide variety of odors and we can easily smell sweet and pleasant scents of ripened fruit and conversely also smell the when a fruit or vegetable is overripe or rotting. This is however not a scalable method to monitor fruits on a large scale in complex agricultural supply chains which instead largely rely on subjective visual inspection. While there exist quantitative tests such as iodine staining to determine the amount of starch that has been converted into sugar, this is a destructive test and does not necessarily indicate the qualities of other fruits in a batch due to the high variance between individuals.

Insect antennae are ideal biological sensors for quantifying these scents. For example fruit flies seek out ripening fruit scents and have antennae that are highly tuned to these odors. A low-cost portable, digital interface could enable a new class of smart devices that could use these highly adapted biological sensors to quantify phenomena such as fruit ripening. Additionally, other insects can sense diseases in foods as well. For example certain

plant diseases and parasites can produce volatile organic compounds that indicates their presence. The high sensitivity of insect antennae from animals such as potato beetles can detect a single diseased potato in a 100 kg sample [43].

3.3 SmellPhone design

3.3.1 Biological odor sensing

A moth's antennae are covered in tiny hair-like sensillum which contain pores allowing airborne odor molecules to enter. The odor molecules bind to specialized odor binding proteins (OBP) which trigger a cascading reaction down the antenna. When many odor molecules are present, this cascading reaction causes an electrical difference between the tip and the base of the antenna. This difference can be measured by specialized circuitry in what is called an electroantennogram (EAG).

3.3.2 Preparation of moth antenna

Manduca sexta moths are reared on a 12 hour day/night cycle. 1-3 day old moths are removed from the rearing chamber and cold-anesthetized for at least 1 hour before the antennae are severed. Severed antennae are able to be used for on average 2 hours and up to 4 hours at room temperature (Fig. 3.3).

The antenna is severed from the moth and approximately 1 mm is trimmed from the tip of the antenna. Two stainless steel wires, approximately 5 mm long and 75 μm diameter, are inserted into each end of the antenna and connected to the electroantennogram circuit.

3.3.3 physical components

The connector between the antenna and the circuit is composed of a 3-pin standard 2.54 mm female round pin header. Two stainless steel wires, 75 μm diameter, are soldered into the first and third pins of the female header, and trimmed so that the wires are approximately 5 mm long. This spacing and length holds the antenna of a *Manduca sexta* antenna in a U-shaped bent position which remains sturdy on both a handheld device and also a flying vehicle for sensing [28].

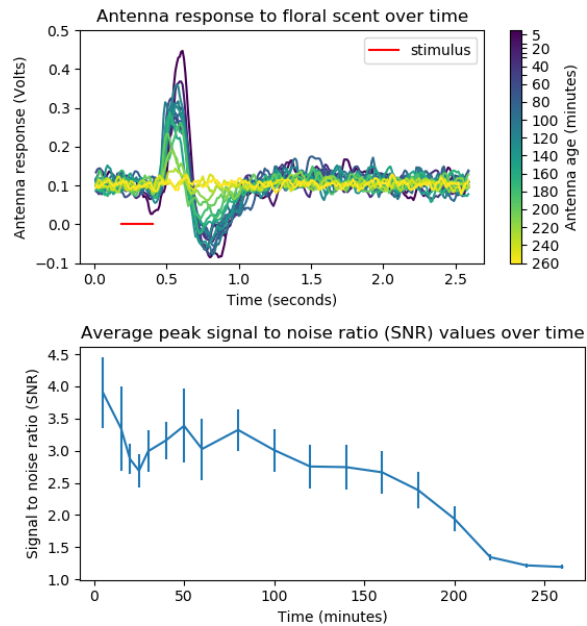


Figure 3.3: Antenna response to floral scent over time.

The SmellPhone is powered by a rechargeable 3.7V 45mAh LIR2032 coin cell battery and is only 3.3 x 1.6 cm not including the audio jack connector. It weighs 9 g and is powered with less than 20 mA at 3.7V. The SmellPhone outputs an analog signal over a standard audio jack connector which interfaces with most cell phones and is compatible with the Backyard Brains (backyardbrains.com) Spike Recorder phone app which allows you to view and record neural spikes.

3.3.4 circuitry

When exposed to floral compounds, the antenna produces a compound electrical potential with a peak-to-peak voltage of approximately tens to hundreds of microVolts. To read this voltage using a standard analog to digital converter, we amplify this signal by 10,000x such that the final peak-to-peak voltage is approximately 0.5-3 Volts. In order to achieve this, we first amplify the antennal signal by 100x in our preamplifier stage (Fig. 3.4). The antenna is subject to baseline drift, so we apply a band pass filter to remove low frequencies (<1

Hz) and frequencies outside of the antennal activity (>10 Hz). After filtering, we amplify the signal 100x in our output amplifier stage.

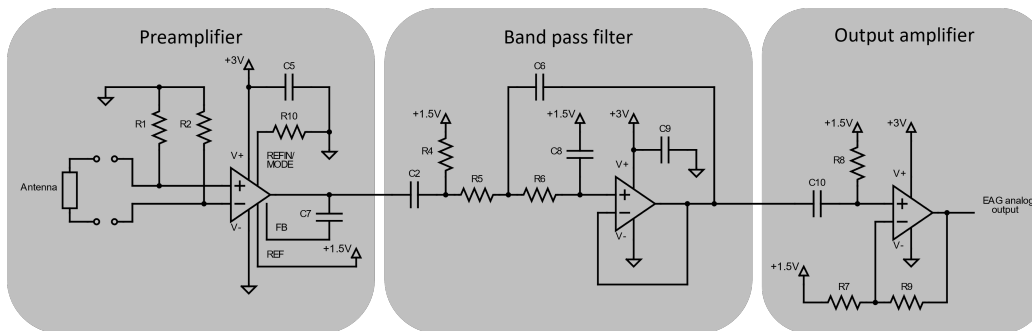


Figure 3.4: The circuitry is comprised of a preamplifier, band pass filter, and output amplifier. It is powered by a 3.7V coin cell battery and a voltage regulator (not shown). The EAG analog output can be read by a cell phone through the audio jack or can be transmitted wirelessly via bluetooth. This circuit is a revised version of the circuit in [28].

3.4 Results

To test the SmellPhone, we stimulate the antenna with a custom floral mixture of compounds present in the flower *Datura wrightii*, [34] a common floral nectar source for *Manduca sexta*. The volume components of this mixture are shown in Table 1 of our previous work [44].

We conduct a test to compare our sensor, the SmellPhone, vs a commercial metal oxide (MOX) sensor, a MiCS-5524 breakout board. We connect both sensors to a National Instruments Data Acquisition Device (NI-DAQ) to record the data and place them in an Omega miniature desktop wind tunnel. The wind speed is set to 2.5 m s^{-1} and stimulant is delivered by the automated odor delivery system in Fig. 3.5. The DAQ controls a solenoid which sends air from an air pump through a clean vial to the front of the wind tunnel. The DAQ sends a signal to switch the solenoid to sending air from the air pump to a vial containing scent and then to the front of the wind tunnel. The scented air is supplied for a period of 200 ms. Various chemical stimulants were used to test both the EAG and MOX sensors shown in Fig. 3.6. Quantities of the chemical sources used are shown in Table 3.1.

Chemical source	Amount
Ethanol	4 mL
Banana	1 g
Tomato	2 g
Floral scent	5 uL
Grapefruit oil	5 uL
Rosemary oil	5 uL
Teatree oil	5 uL

Table 3.1: Chemical source amounts. The floral scent, grapefruit oil, rosemary oil, and teatree oil were each deposited on filter paper and placed into the scent vial.

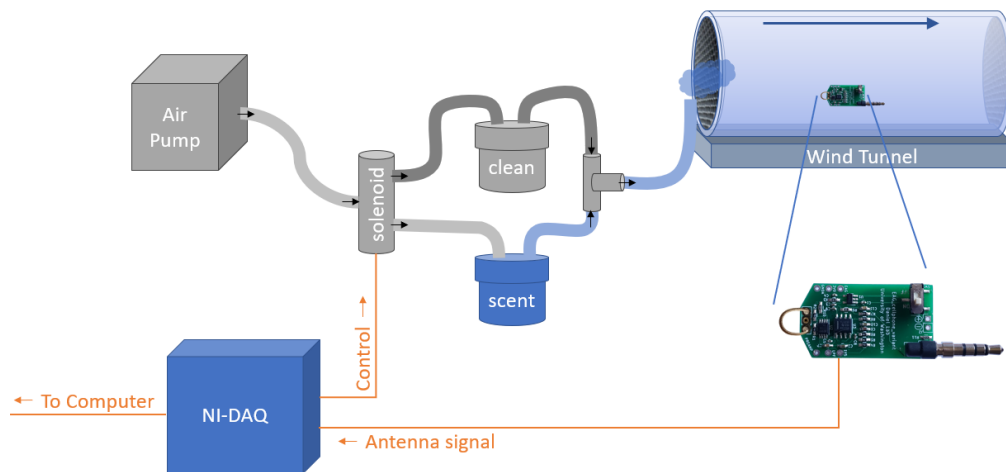


Figure 3.5: The automated odor delivery system. The National Instruments Data Acquisition Device (NI-DAQ) switches the solenoid between supplying clean air or scented air to the front of the wind tunnel. A controlled stimulus of scented air travels through the wind tunnel and across the electroantennogram (EAG) which sends the antenna signal to the DAQ for recording.

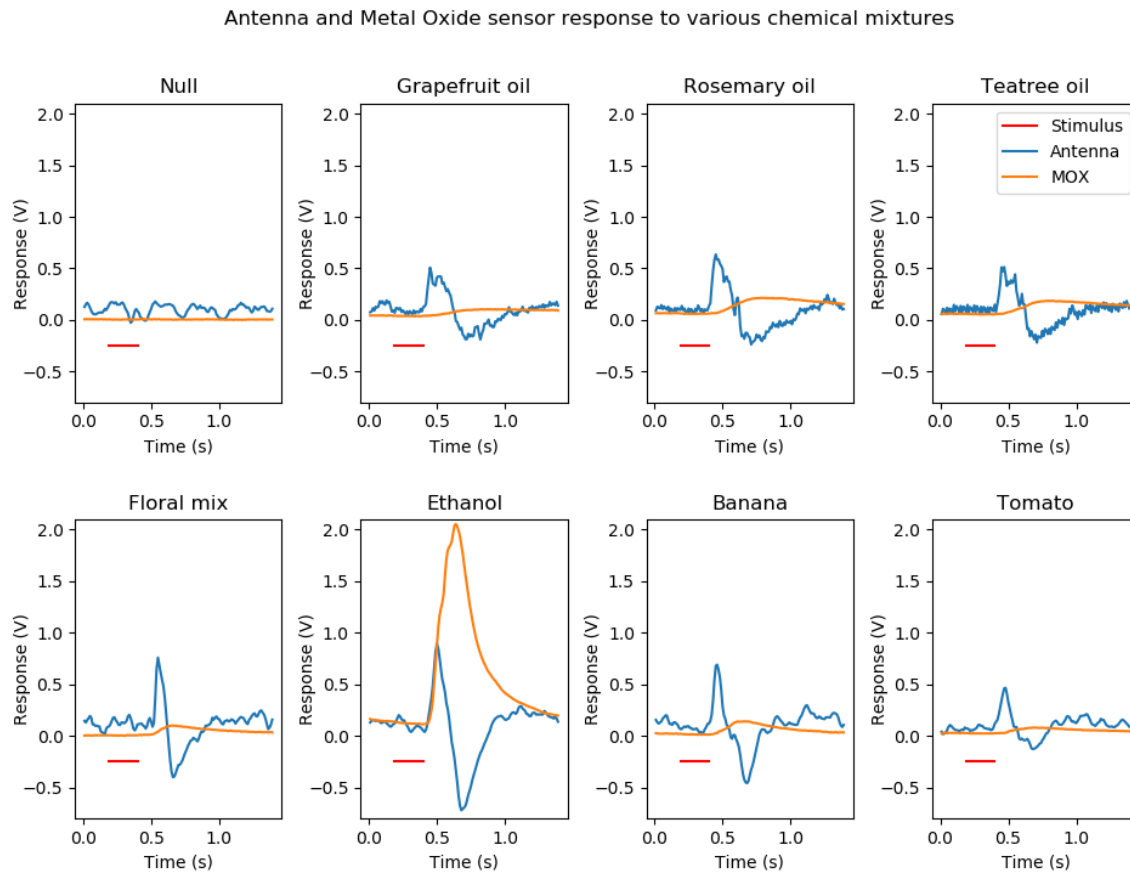


Figure 3.6: A comparison of our electroantennogram (EAG) sensor vs a commercial metal oxide (MOX) sensor.

Seven different scents were tested including 4 mL 95% ethanol, 1 g banana pieces, 2 g tomato pieces, and 5 μ L of the following chemicals each deposited on a small piece of filter paper and then inserted into the vial: floral mix [28], grapefruit essential oil, rosemary essential oil, and teatree essential oil.

The time for the scent to travel from the source located in the scented vial to reach the sensors placed in the wind tunnel was calculated to be approximately 200 ms. This was verified by using dry ice as the source to produce a visible stimulus. The solenoid was triggered and a camera was placed to record when the stimulus reached the sensors located inside the wind tunnel. In the plots shown in Fig. 3.6, each stimulus was for exactly 200

ms, so the time when the stimulus reaches the sensors approximately coincides with trailing end of the stimulus marker in the plots.

In the top left plot of Fig. 3.6 is a null trial where a clean vial was used in place of the scented vial. The activity in the antenna in the null trial may be explained by various smells present in the space since the experiments were not conducted in a sterile space. However, you can see that there is no extra activity in the antenna from the switched stimulus to the clean vial in the null trial.

In the remaining plots, the antenna produces a visible response to the stimulus. The metal oxide sensor (MOX) produces a weak response to all chemicals except for ethanol. In all trials, the time to the peak of the response in the antenna is quicker than the time to peak of the response for the MOX sensor. Additionally, the recovery time of the antenna is quicker than the MOX sensor.

The same circuitry used for the SmellPhone can also be adapted to interface with a small flying platform for autonomous odor localization. In previous work [44], we have shown that our custom electroantennogram circuitry on a palm-sized drone, dubbed the Smellicopter, can autonomously navigate to the source of an odor plume inside of a wind tunnel with and without the presence of obstacles using a bio-inspired search algorithm.

BIBLIOGRAPHY

- [1] P. P. Neumann, V. H. Bennetts, A. J. Lilienthal, M. Bartholmai, and J. H. Schiller, “Gas source localization with a micro-drone using bio-inspired and particle filter-based algorithms,” *Advanced Robotics*, vol. 27, pp. 725–738, 6 2013.
- [2] B. Luo, Q.-H. Meng, J.-Y. Wang, and M. Zeng, “A flying odor compass to autonomously locate the gas source,” *IEEE Transactions on Instrumentation and Measurement*, pp. 1–13, 2017.
- [3] D. Martinez, L. Arhidi, E. Demondion, J.-B. Masson, and P. Lucas, “Using insect electroantennogram sensors on autonomous robots for olfactory searches,” *Journal of Visualized Experiments*, 8 2014.
- [4] J. A. Riffell, L. Abrell, and J. G. Hildebrand, “Physical processes and real-time chemical measurement of the insect olfactory environment,” *Journal of Chemical Ecology*, vol. 34, pp. 837–853, 7 2008.
- [5] S. Anton and B. S. Hansson, “Sex pheromone and plant-associated odour processing in antennal lobe interneurons of male *spodoptera littoralis* (lepidoptera: Noctuidae),” *Journal of Comparative Physiology A 1995 176:6*, vol. 176, pp. 773–789, 6 1995.
- [6] M. A. Willis, E. A. Ford, and J. L. Avondet, “Odor tracking flight of male *manduca sexta* moths along plumes of different cross-sectional area,” *Journal of Comparative Physiology A*, vol. 199, pp. 1015–1036, 11 2013.
- [7] N. Voges, A. Chaffiol, P. Lucas, and D. Martinez, “Reactive searching and infotaxis in odor source localization,” *PLoS Computational Biology*, vol. 10, p. e1003861, 10 2014.
- [8] C. E. Reisenman, J. A. Riffell, E. A. Bernays, and J. G. Hildebrand, “Antagonistic effects of floral scent in an insect–plant interaction,” *Proceedings of the Royal Society B: Biological Sciences*, vol. 277, pp. 2371–2379, 8 2010.
- [9] D. Harvey, T.-F. Lu, and M. Keller, “Comparing insect-inspired chemical plume tracking algorithms using a mobile robot,” *IEEE Transactions on Robotics*, vol. 24, pp. 307–317, 4 2008.
- [10] R. Pang, F. van Breugel, M. Dickinson, J. A. Riffell, and A. Fairhall, “History dependence in insect flight decisions during odor tracking,” *PLoS Computational Biology*, vol. 14, pp. 1–26, 02 2018.

- [11] M. Vergassola, E. Villermaux, and B. I. Shraiman, “‘infotaxis’ as a strategy for searching without gradients,” *Nature*, vol. 445, pp. 406–409, 1 2007.
- [12] H. M. Herr and A. M. Grabowski, “Bionic ankle-foot prosthesis normalizes walking gait for persons with leg amputation,” *Proceedings. Biological sciences*, vol. 279, pp. 457–464, 2012.
- [13] J. Herron, T. Denison, and H. Chizeck, “Closed-loop dbs with movement intention,” *International IEEE/EMBS Conference on Neural Engineering, NER*, vol. 2015, pp. 844–847, 07 2015.
- [14] M. W. Gander, J. D. Vrana, W. E. Voje, J. M. Carothers, and E. Klavins, “Digital logic circuits in yeast with crispr-dcas9 nor gates,” *Nature Communications 2017 8:1*, vol. 8, pp. 1–11, 5 2017.
- [15] L. Ricotti, B. Trimmer, A. W. Feinberg, R. Raman, K. K. Parker, R. Bashir, M. Sitti, S. Martel, P. Dario, and A. Menciassi, “Biohybrid actuators for robotics: A review of devices actuated by living cells,” *Science Robotics*, vol. 2, no. 12, p. eaaq0495, 2017.
- [16] N. W. Xu and J. O. Dabiri, “Low-power microelectronics embedded in live jellyfish enhance propulsion,” *Science Advances*, vol. 6, p. eaaz3194, 1 2020.
- [17] C. Lahondère, C. Vinauger, R. P. Okubo, G. H. Wolff, J. K. Chan, O. S. Akbari, and J. A. Riffell, “The olfactory basis of orchid pollination by mosquitoes,” *Proceedings of the National Academy of Sciences of the United States of America*, vol. 117, pp. 708–716, 1 2020.
- [18] S. A. Budick and M. H. Dickinson, “Free-flight responses of drosophila melanogaster to attractive odors,” *Journal of Experimental Biology*, vol. 209, pp. 3001–3017, 8 2006.
- [19] A. Mafra-Neto and R. T. Cardé, “Fine-scale structure of pheromone plumes modulates upwind orientation of flying moths,” *Nature*, vol. 369, pp. 142–144, 1994.
- [20] S. Shigaki, M. R. Fikri, and D. Kurabayashi, “Design and experimental evaluation of an odor sensing method for a pocket-sized quadcopter,” *Sensors*, vol. 18, no. 11, 2018.
- [21] J. Burgués, V. Hernández, A. Lilienthal, and S. Marco, “Smelling nano aerial vehicle for gas source localization and mapping,” *Sensors*, vol. 19, p. 478, 1 2019.
- [22] B. P. Duisterhof, S. Krishnan, J. J. Cruz, C. R. Banbury, W. Fu, A. Faust, G. C. H. E. de Croon, and V. J. Reddi, “Learning to seek: Deep reinforcement learning for phototaxis of a nano drone in an obstacle field,” 9 2019.

- [23] M. Spehr and S. D. Munger, “Olfactory receptors: G protein-coupled receptors and beyond,” *Journal of Neurochemistry*, vol. 109, pp. 1570–1583, 6 2009.
- [24] Y. Kuwana, S. Nagasawa, I. Shimoyama, and R. Kanzaki, “Synthesis of the pheromone-oriented behaviour of silkworm moths by a mobile robot with moth antennae as pheromone sensors,” *Biosensors and Bioelectronics*, vol. 14, pp. 195–202, 2 1999.
- [25] N. Ando and R. Kanzaki, “Using insects to drive mobile robots — hybrid robots bridge the gap between biological and artificial systems,” *Arthropod Structure Development*, vol. 46, pp. 723–735, 9 2017.
- [26] J. V. Huang, Y. Wei, and H. G. Krapp, “A biohybrid fly-robot interface system that performs active collision avoidance,” *Bioinspiration Biomimetics*, vol. 14, p. 065001, 9 2019.
- [27] B. Lan, R. Kanzaki, and N. Ando, “Dropping counter: A detection algorithm for identifying odour-evoked responses from noisy electroantennograms measured by a flying robot,” *Sensors (Basel, Switzerland)*, vol. 19, 10 2019.
- [28] M. J. Anderson, J. G. Sullivan, J. L. Talley, K. M. Brink, S. B. Fuller, and T. L. Daniel, “The “smellicopter,” a bio-hybrid odor localizing nano air vehicle,” in *2019 IEEE/RSJ International Conference on Intelligent Robots and Systems (IROS)*, pp. 6077–6082, 2019.
- [29] R. A. Fandino, A. Haverkamp, S. Bisch-Knaden, J. Zhang, S. Bucks, T. A. T. Nguyen, K. Schröder, A. Werckenthin, J. Rybak, M. Stengl, M. Knaden, B. S. Hansson, and E. Groe-Wilde, “Mutagenesis of odorant coreceptor orco fully disrupts foraging but not oviposition behaviors in the hawkmoth *manduca sexta*,” *Proceedings of the National Academy of Sciences of the United States of America*, vol. 116, pp. 15677–15685, 7 2019.
- [30] S. B. Fuller, A. D. Straw, M. Y. Peek, R. M. Murray, and M. H. Dickinson, “Flying drosophila stabilize their vision-based velocity controller by sensing wind with their antennae,” *Proceedings of the National Academy of Sciences of the United States of America*, vol. 111, pp. E1182–E1191, 4 2014.
- [31] S. P. Sane, A. Dieudonné, M. A. Willis, and T. L. Daniel, “Antennal mechanosensors mediate flight control in moths,” *Science*, vol. 315, pp. 863–866, 2 2007.
- [32] J. K. Lee and N. J. Strausfeld, “Structure, distribution and number of surface sensilla and their receptor cells on the olfactory appendage of the male moth *manduca sexta*,” *Journal of Neurocytology* 1990 19:4, vol. 19, pp. 519–538, 8 1990.
- [33] S. P. Sane and N. P. Jacobson, “Induced airflow in flying insects ii. measurement of induced flow,” *Journal of Experimental Biology*, vol. 209, pp. 43–56, 1 2006.

- [34] C. E. Reisenman, J. A. Riffell, K. Duffy, A. Pesque, D. Mikles, and B. Goodwin, “Species-specific effects of herbivory on the oviposition behavior of the moth *manduca sexta*,” *Journal of Chemical Ecology*, vol. 39, pp. 76–89, 1 2013.
- [35] W. Tsang, A. L. Stone, D. Otten, Z. N. Aldworth, T. L. Daniel, J. G. Hildebrand, R. B. Levine, and J. Voldman, “Insect-machine interface: A carbon nanotube-enhanced flexible neural probe,” *Journal of Neuroscience Methods*, vol. 204, no. 2, pp. 355–365, 2012.
- [36] D. C. Daly, P. P. Mercier, M. Bhardwaj, A. L. Stone, Z. N. Aldworth, T. L. Daniel, J. Voldman, J. G. Hildebrand, and A. P. Chandrakasan, “A pulsed uwb receiver soc for insect motion control,” *IEEE Journal of Solid-State Circuits*, vol. 45, no. 1, pp. 153–166, 2010.
- [37] Y. Li, J. Wu, and H. Sato, “Feedback control-based navigation of a flying insect-machine hybrid robot,” *Soft Robotics*, vol. 5, no. 4, pp. 365–374, 2018. PMID: 29722607.
- [38] H. Sato, C. W. Berry, Y. Peeri, E. Baghoomian, B. E. Casey, G. Lavella, J. M. Vanden-Brooks, J. F. Harrison, and M. M. Maharbiz, “Remote radio control of insect flight,” *Frontiers in Integrative Neuroscience*, vol. 3, p. 24, 10 2009.
- [39] V. Shields and J. Hildebrand, “Responses of a population of antennal olfactory receptor cells in the female moth *manduca sexta* to plant-associated volatile organic compounds,” *Journal of Comparative Physiology A: Sensory, Neural, and Behavioral Physiology*, vol. 186, pp. 1135–1151, 2 2001.
- [40] B. S. Hansson, M. A. Carlsson, and B. Kalinovà, “Olfactory activation patterns in the antennal lobe of the sphinx moth, *manduca sexta*,” *Journal of Comparative Physiology A 2003 189:4*, vol. 189, pp. 301–308, 3 2003.
- [41] A. M. Fraser, W. L. Mechaber, and J. G. Hildebrand, “Electroantennographic and behavioral responses of the sphinx moth *manduca sexta* to host plant headspace volatiles,” *Journal of Chemical Ecology*, vol. 29, pp. 1813–1833, 2003.
- [42] M. M. Ali, N. Hashim, S. Abd Aziz, and O. Lasekan, “Principles and recent advances in electronic nose for quality inspection of agricultural and food products,” *Trends in Food Science & Technology*, vol. 99, pp. 1–10, 2020.
- [43] S. Schütz, B. Weißbecker, U. Koch, and H. Hummel, “Detection of volatiles released by diseased potato tubers using a biosensor on the basis of intact insect antennae,” *Biosensors and Bioelectronics*, vol. 14, no. 2, pp. 221–228, 1999.
- [44] M. J. Anderson, J. G. Sullivan, T. K. Horiuchi, S. B. Fuller, and T. L. Daniel, “A bio-hybrid odor-guided autonomous palm-sized air vehicle,” *Bioinspiration & Biomimetics*, vol. 16, p. 026002, mar 2020.

Appendix A

WHERE TO FIND THE FILES

Please contact Melanie Anderson (melaniea360@gmail.com) to receive files.